Journal of Earthquake Engineering
Vol. 9, Special Issue 2 (2005) 355–393

Imperial College Press
www.icpress.co.uk

A KINEMATIC INTERACTION MODEL FOR A LARGE-DIAMETER SHAFT FOUNDATION. AN APPLICATION TO SEISMIC DEMAND ASSESSMENT OF A BRIDGE SUBJECT TO COUPLED SWAYING-ROCKING EXCITATION

CARLO BELTRAMI*

European School of Advanced Studies in Reduction of Seismic Risk (ROSE School)
Università degli Studi di Pavia, c/o Collegio A. Volta
Via Ferrata 17, 27100 Pavia, Italy
carlo.beltrami@rcm.inet.it

CARLO G. LAI

European Centre for Training and Research in Earthquake Engineering (EUCENTRE)
c/o Dipartimento di Meccanica Strutturale, Università degli Studi di Pavia
Via Ferrata 1, 27100 Pavia, Italy

ALAIN PECKER

Géodynamique et Structure, 157, rue des Blains, 92 220 Bagneux, France
Laboratory of Solid Mechanics Ecole Polytechnique, 91 128 Palaiseau, France

The aim of this paper is to illustrate an analytical model for the assessment of kinematic interaction of large-diameter shaft foundations. The model is derived using recently obtained solutions of soil structure interaction problems of rigid walls and fixed base cylinders subjected to a dynamic excitation. The proposed model constitutes an extension to a deformable base of the elastodynamic solution of a rigid, fixed-base cylinder imbedded in a homogeneous or inhomogeneous soil stratum with different lateral boundary conditions. The analytical model has been validated by means of a finite elements code and it has been implemented in a consistent seismic soil-structure-interaction analysis procedure. An application of the model to a long, multi-span continuous prestressed concrete viaduct with tall piers has been carried out focusing on the importance of kinematic interaction. The main finding of the study is that the foundation input motion is characterised not only by a translational horizontal component which is usually of a reduced amplitude if compared with the free-field ground motion, but also by a rotational component that is responsible for a large seismic demand in the superstructure. The proposed model represents an effective tool to be used in the engineering practice to assess both the seismic actions induced by the ground shaking on the foundation system and the effective input motion of a superstructure founded on massive and large diameter shafts.

Keywords: Kinematic interaction; dynamic soil structure interaction; soil dynamics; deep foundations; seismic bridge analysis and design.

*Corresponding author address: Via D. Cimarosa 12/5, 20144 Milan, Italy.

1. Introduction

The importance of evaluating the effects of seismic Soil-Foundation-Structure Interaction (SFSI) in case of deep and massive foundations systems is well established in modern seismic codes [e.g. EC8] even though the approach traditionally used in engineering practice to account for the problem is often oversimplified and mostly involves modelling the static deformability of the ground.

In general, a rigorous assessment of seismic SFSI is not a simple task particularly for structures founded on deep foundations because of the difficulties associated with the evaluation of kinematic interaction and scattering effects. Therefore a solution to this problem that is capable of offering a satisfactory trade-off between rigor and simplicity is highly desirable especially in standard engineering practice. The study illustrated in this paper and described in more detail in the work by Beltrami [2004] attempts to make a contribution in this direction with regards to structures founded on large-diameter shaft foundations such as those widely used for instance in multi-span continuous viaducts.

It should be emphasised that the interest in studying the seismic SFSI is motivated not only by the need to satisfy certain geotechnical requirements (e.g. bearing capacity assessment, settlement calculation, etc.) related to foundation response to earthquake loading, but also by the necessity of computing the "effective" earthquake excitation to a structure (which is also called the Foundation Input Motion or FIM) with respect to the free-field ground motion. The latter strongly influences the structural seismic demand as it takes into account both the soil-foundation coupling (i.e. the dynamic impedance function of the soil-foundation system) and the scattering effects caused by the motion of embedded foundations (i.e. the kinematic interaction effects). It is rather unfortunate that kinematic interaction effects are often neglected in engineering practice due to the difficulties of their evaluation even though they may be relevant.

The type of foundation considered in this study is a large-diameter shaft, that is a massive cylindrical end-bearing foundation made of cast in-place reinforced concrete (see Fig. 1). For important bridges the typical size ranges from 6 to 12 m diameter and 35 to 40 m length. Use of this foundation type for bridge structures is fairly common particularly at sites where soil conditions do not permit the use of driven piles or it is economically more convenient to replace a group of drilled piles with a single, large-diameter drilled shaft which also obviates the need for a pile cap. Furthermore, drilled shaft foundations are employed to support heavy loads as they minimise the settlements, or alternatively to carry uplift and lateral loads (as it occurs for earthquake loading).

Although the literature on seismic response of deep foundations is fairly extensive where it concerns flexible piles,[†] relatively few solutions are available for the

[†]With the pioneer studies of dynamic soil-pile interaction carried out in the 60s and continued until today in refined numerical models (using finite element or boundary element methods) or simplified analytical solutions such as the Beam-on-Dynamic-Winkler-Foundation (BDWF) models.

Fig. 1. Excavation of a large diameter drilled shaft (photo courtesy by Ulrich Hegg Eng. MSc., Milan).

case of deep, large-diameter shafts, even if they are frequently used for instance in long, multi-span viaducts. The seismic performance and damage suffered by flexible piles has been the subject of post-earthquake investigations and reconnaissance reports of several major earthquakes that have occurred in the past. Unfortunately fewer case histories are available for large-diameter shafts. One reason may be attributed to the fact that these types of foundations are characterised by a large bearing capacity which is not overcome even when subjected to earthquake loading. Consequently geotechnical collapse of large-diameter shafts is rarely observed in practice as their design is generally governed by the serviceability rather than the ultimate limit state. Another factor that may be responsible of the limited number of failures observed in post-earthquake investigations of large-diameter shafts is the particular type of structures that adopt this type of deep foundation in comparison with flexible piles.

2. Kinematic Interaction in Seismic Soil-Structure Interaction Problems

For a structure subjected to earthquake loading the Soil-Foundation-Structure Interaction (SFSI) problem involves assessment of the dynamic response of the complete structural system under dynamic loading which originates in the interior of a soil medium and is transmitted to the structure through its foundations. The solution of the overall SFSI problem is usually decomposed into the following steps

[Caltrans, 1999; Steward *et al.*, 1998; Pecker, 1984, 2002]:

(i) Computation of the *dynamic impedance matrix* of the soil-foundation system. This is a frequency-dependent, complex-valued array quantifying the stiffness and damping characteristics of the foundation-soil interaction. Damping, which is represented by the imaginary part of the dynamic impedance function, is caused by two different energy dissipation mechanisms: The first is due to the hysteretic response of the soil medium and foundation system, the second is due to the geometric radiation of seismic energy away from the foundation through the soil medium.

(ii) Computation of the so-called Foundation Input Motion (FIM) that is the "*true*" motion experienced by the superstructure if the latter had no mass. This step is related with the assessment of the *kinematic interaction* or *scattering* effects which are due to the inability of the foundation, owing to its stiffness, to conform to the free-field ground motion.

(iii) Computation of internal actions at the foundation base generated by the inertial forces developed in the structure due to its own vibrations. This step refers to the evaluation of the *inertial interaction* effects which cause displacements and rotations of the foundation base to be different from FIM.

(iv) Computation of the *foundation capacity* that is determining the resistance of the soil-foundation system to earthquake loading.

In implementing these steps for the seismic design of piles it has been a common practice until recent years to take into account only the inertial interaction effects, namely the inertial loads generated by superstructure's mass caused by the seismic excitation.

Mizuno [1987] was the first researcher who observed during post-earthquake investigations of major events that some slender piles failures where located at depths distant from the pile top and occurred in soil deposits that did not suffer ground failure (such as liquefaction) or severe mechanical degradation during the earthquake. Mizuno also noticed that pile damage occurred at the same locations where soil had experienced large deformations due to ground shaking which often coincided with zones characterised by sharp stiffness discontinuities in the soil profile. This geometric condition imposed on piles by the surrounding soil is responsible for the generation of large bending moments. These arise from the curvature induced by the reflection and refraction pattern of seismic waves in correspondence to the shear modulus discontinuity of the medium profile.

This soil-pile deformation governed by the dynamic response of the system formed by the pile and the surrounding soil to earthquake loading is named "*kinematic interaction*" and it has been explicitly introduced for the first time ever in a seismic code by Eurocode 8, Part 5. Extensive studies into the subject have been carried out during the last two decades by several researchers including Kagawa *et al.* [1980], Gazetas [1984], Dobry *et al.* [1988], Nogami *et al.* [1992], Kavvadas

et al. [1993], Pender [1993], Mylonakis *et al.* [1997, 2000], El Naggar *et al.* [1999] and Nikolaou *et al.* [2001], just to name a few. These works provide valuable contributions and simplified analytical methods to account for the kinematic interaction of slender piles such as the Beam-on-Dynamic-Winkler-Foundation (BDWF) model.

In general, the methods used to perform seismic SFSI analyses can be subdivided into *direct* and *substructure* approaches. In the *direct* approach the structure, the foundation with the surrounding unbounded soil are included within the same numerical model and the dynamic analysis of the whole system is carried out in a single step by a time-integration of the equations of motion. This approach is computationally expensive as it requires 3D dynamic modelling of structures founded on unbounded media at relatively high frequencies. As a result the direct approach is employed only for very important projects such as nuclear power plants, suspended bridges, etc.

Conversely with the *substructure* approach [Kausel *et al.*, 1978], the SFSI problem is decomposed into three distinct sub-problems which are solved independently (see Fig. 2). The substructure approach implicitly assumes the validity of the superposition principle and thus presumes that the structure, the foundation and the soil exhibit a linear mechanical response to earthquake loading. It has been shown however that this methodology is successfully applicable also to equivalent-linear and moderately non-linear systems [Mylonakis *et al.*, 1997; Caltrans, 1999]. The principal advantage of the substructure approach is its flexibility and ease of implementation in engineering practice.

Large diameter shaft foundations are essentially rigid cylinders that are not expected to induce very large nonlinearities in the surrounding soil during seismic shaking. Thus they are well suited to be studied within the framework of the superposition's theorem and the substructure approach.

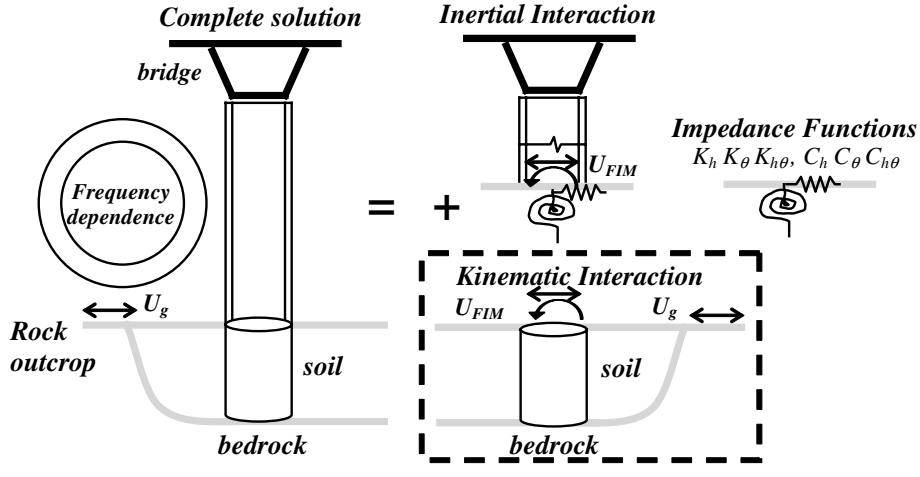

Fig. 2. The Superposition Theorem, framework of the present kinematic interaction model.

3. A Kinematic Interaction Model for Large Diameter Shaft Foundations

The starting point to study kinematic interaction in piled foundations is the definition of dynamic pressures exerted by soil around the surface of the pile. It is assumed the validity of the small-strain theory and that the soil behaves like a linear, one-constituent, viscoelastic material.

Recent studies by Veletsos and Younan [1994–1995] have made important contributions to the solution of a closely related problem which is that of viscoelastic dynamic pressures exerted by soils to rigid and flexible retaining walls. Of particular interest is the solution obtained for the case of massive gravity walls or basement walls braced at both top and bottom where the wall movement is not sufficient to fully mobilise the shear resistance of the backfill.

This case has analogies with the dynamic response to earthquake loading of a large diameter shaft foundation. The main difference is in the geometry of the two problems, which is two-dimensional for the earth-retaining wall and three-dimensional for the large-diameter shaft foundation.

The dynamic pressures exerted by soil around the surface of a vertical, rigid cylinder have been originally computed by Tajimi [1969] and Veletsos and Younan [1994, 1995]. Their result will be used in this study as a basis for the construction of an analytical model aimed at evaluating the kinematic interaction of a large-diameter cylinder embedded in a viscoelastic medium and resting on a deformable base. The basic assumptions made in this study concerning the geometry of the foundation and soil constitutive model are as follows:

(i) Foundation geometry and stiffness: Rigid circular cylinder of radius R embedded in a soil layer of constant thickness H and infinite extent in the horizontal plane (no topographic effects);
(ii) Constitutive model of soil layer and bedrock: Idealisation of the medium as a linear viscoelastic material with frequency-independent properties: Mass density ρ, shear modulus G, Poisson's ratio ν, and material damping ratio D. Damping and shear modulus are strain-compatible with the level of excitation by a preliminary equivalent-linear response analysis of the stratum;
(iii) Excitation: Both the base of the cylinder and the layer are considered to undergo a space-invariant, uniform horizontal motion.

Furthermore the soil was assumed to deform according to the *plane-stress* hypothesis as it was originally proposed by Veletsos and Younan [1995] for a better representation of the displacement field around a large-diameter pile with respect to the *plane-strain* assumption originally proposed by Tajimi [1969] in a pioneer work on the same subject.

The latter hypothesis was shown to be more appropriate for slender piles. The plane-stress assumption implies vanishing of the normal stress field in the vertical direction of the soil medium as opposed to vanishing of the vertical displacement

as assumed in the plane-strain case. Plane-stress has also the advantage of leading to more stable numerical solutions for values of the Poisson ratio ν approaching 0.5 (incompressible material).

An important contribution to the problem of dynamic soil-structure interaction of a rigid cylinder was given by Veletsos and Younan [1995] who computed the dynamic pressures exerted along the surface of a cylinder fixed at the base by a soil modelled as a viscoelastic medium. The system is excited by a vertically propagating, horizontally polarised, harmonic shear SH wave. Their solution is based on the classical Baranov-Novak (BN) idealisation of the medium, where the soil is represented by a series of independent thin layers with a circular hole placed at the centre of the system. The shear stiffness of each thin layer is given by its dynamic impedance K (for a detailed description of the Baranov-Novak model see [Veletsos and Dotson, 1988]). In the far-field the BN layers behave as a cantilever shear beam, therefore similar to the well-known Scott's model for rigid walls.

Veletsos and Younan [1995] have shown that for this model the resulting horizontal dynamic force per unit height of the cylinder originated by a uniform, harmonic acceleration at the base $\ddot{x}_g(t) = \ddot{X}_g e^{i\omega t}$ is simply given by the product of the layers' mechanical impedance K and the difference between the horizontal displacement computed at the shear beam far-field and the cylinder centre axis. This approach of calculating the dynamic force along the cylinder is very efficient and it has the advantage of being characterised by a small number of lumped parameters. For this reason it is adopted in this study in extending the solution obtained by Veletsos and Younan [1995] to the case of a cylinder placed on a deformable base.

In order to overcome some of the flaws of the BN model when applied to large-diameter shafts, Veletsos and Younan [1995] have proposed an improvement based on the concept of "*constrained layers*" which add a capacity of the medium between the far-field and the cylinder to transfer forces vertically by means of horizontal shearing actions. The basic idea of the constrained layers is to add at each BN thin layer a system of massless linear springs (elastic constraints) equally directed along the two horizontal radial u and circumferential ν directions (see Fig. 3). The improvement suggested by Veletsos and Younan [1995] is based on the assumption of negligible lateral variations of the vertical displacement in the medium, which is equivalent assuming 1D wave propagation. These additional springs can simply be interpreted as forces per unit area and are in magnitude proportional to modal displacements and thus independent of position and are functions only of the modal number 'n':

$$k_n^* = \rho\omega_n^2 = \left[\frac{(2n-1)\pi}{2}\right]^2 \frac{G}{H^2}. \tag{1}$$

After including between the BN thin layers these additional elastic springs one can then compute the modified horizontal impedance of the layer. The governing equations of motion written in radial and circumferential coordinates will now include the additional terms k_n^* denoting the elastic constraints in the two horizontal

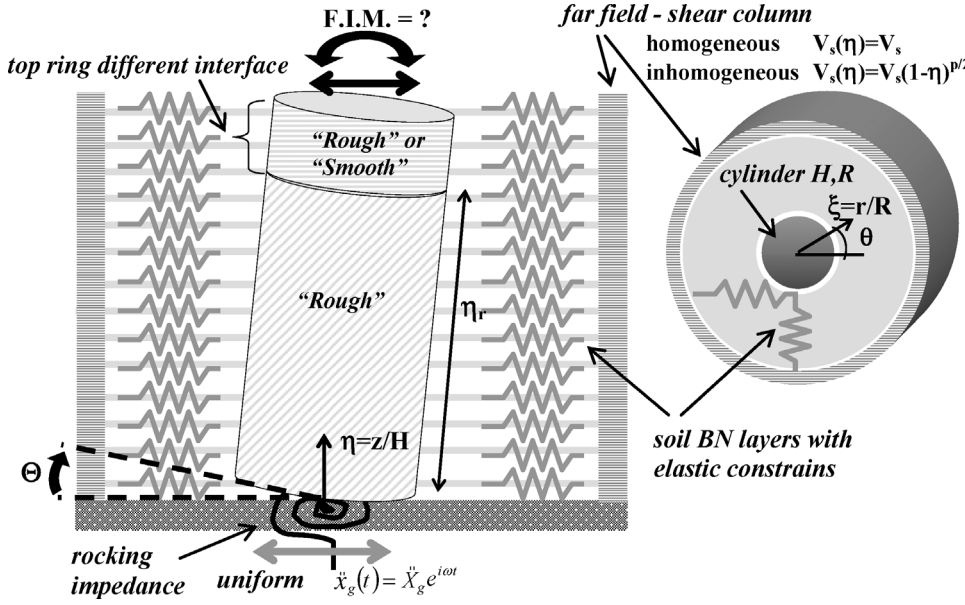

Fig. 3. Schematic view of the model used to study the soil-foundation kinematic interaction problem.

directions:

$$\frac{1}{R}\left(\frac{\partial \sigma_r}{\partial \xi} + \frac{1}{\xi}\frac{\partial \tau_{r\theta}}{\partial \theta} + \frac{\sigma_r - \sigma_\theta}{\xi}\right) = \rho\frac{\partial^2 u}{\partial t^2} + k_n^* u, \tag{2}$$

$$\frac{1}{R}\left(\frac{\partial \tau_{r\theta}}{\partial \xi} + \frac{1}{\xi}\frac{\partial \sigma_\theta}{\partial \theta} + \frac{2}{\xi}\tau_{r\theta}\right) = \rho\frac{\partial^2 v}{\partial t^2} + k_n^* v. \tag{3}$$

Following the development by Veletsos and Dotson [1988] the impedance of the BN layers may be computed by determining in the frequency domain the displacements u and v using the method of potential functions.

Knowing the expression of the displacements u and v at the lateral soil-foundation interface, it is possible to compute the expressions of the normal stress, that in Beltrami [2004] has been corrected from the one published by the original authors [Veletsos and Younan, 1995]:

$$\sigma(1) = \left(\frac{2\Lambda^* G^*}{\Lambda^* + 2G^*} + \frac{2G^*}{R}\right)\{A[(2+\mu^2)K_1(\mu) + \mu K_0(\mu)] - B[2K_1(\lambda) + \lambda K_0(\lambda)]\}, \tag{4}$$

and of the shearing circumferential stress:

$$\tau(1) = \frac{G^*}{R}\{A[2K_1(\mu) + \mu K_0(\mu)] - B[(2+\lambda^2)K_1(\lambda) + \lambda K_0(\lambda)]\}, \tag{5}$$

where K_0 and K_1 are the modified Bessel functions of second kind of order 0 and 1 respectively and A and B are constants of integration derived from boundary

conditions. The terms $\Lambda^* = 2\nu G^*/(1-2\nu)$, $\varepsilon_0 = \sqrt{2/(1-\nu)}$ are elastic constants and $\lambda = \sqrt{s_n^2 - a_0^2/(1+i\delta)}$, $\mu = \lambda/\varepsilon_0$ are frequency-dependent ($a_0 = \omega R/V_s$) complex-valued parameters (coefficients) which are functions of the layer elastic constraint $s_n = \sqrt{k_n^* R^2/G^*}$. The superscript "*" is used to denote a complex-valued quantity, and $\delta = 2D$.

The constants of integration A and B are obtained from boundary conditions which are continuity of normal and tangential circumferential displacements at the soil-cylinder interface. Their values are [Beltrami, 2004]:

$$\begin{aligned} A &= -[2K_1(\lambda) + \lambda K_0(\lambda)]/\Delta \quad B = -[2K_1(\mu) + \mu K_0(\mu)]/\Delta \\ \Delta &= [K_1(\mu) + \mu K_0(\mu)] \cdot [K_1(\lambda) + \lambda K_0(\lambda)] - K_1(\mu) K_1(\lambda). \end{aligned} \tag{6}$$

Finally the impedance K_n of the elastically constrained layer may be computed by integrating the normal and tangential stress components over the lateral surface of a cylinder of unit height:

$$K_n = -\int_0^{2\pi} [\sigma(1)\cos(\theta)^2 - \tau(1)\sin(\theta)^2] R d\theta = -\pi R[\sigma(1) - \tau(1)]. \tag{7}$$

This expression is instructive because it shows separately the contributions to K_n of normal and shear dynamic stresses. It should also be observed that the layer impedance K_n is modal dependent and thus it is calculated for each mode differently.

To generalize the soil-structure interaction model of a rigid cylinder developed by Veletsos and Younan [1995] to the case of a cylinder resting on a deformable rather than fixed base, it is necessary to define the harmonic rotation at the base of the cylinder as well as the horizontal displacement field along the central axis of the cylinder. The instantaneous value of the cylinder rotation (counted positive clockwise) and the horizontal displacement of the cylinder at the dimensionless distance $\eta = z/H$ from the base is given by the following rigid body motion relations:

$$\Theta(t) = \bar{\Theta} e^{i\omega t}, \tag{8}$$

$$U_r(\eta, t) = \bar{\Theta} \eta H \cdot e^{i\omega t}. \tag{9}$$

Expanding $U_r(\eta, t)$ in terms of the natural modes of vibration of the stratum one obtains:

$$U_r(\eta, t) = \sum_{n=1}^{N_{max}} W_n \sin\left[\frac{(2n-1)\pi}{2}\eta\right] \cdot e^{i\omega t}, \tag{10}$$

where N_{max} is the total number of modes that are accounted for in the calculation. Now it is easy to compute the horizontal dynamic force per unit height of the cylinder from the superposition of N_{max} modes of vibration of the stratum modelled as a shear beam, multiplied by the difference between the horizontal displacement

U_n computed in the far-field and the contribution from the rocking base W_n. The result is:

$$F(\eta, t) = \sum_{n=1}^{N_{max}} K_n (U_n - W_n) \sin\left[\frac{(2n-1)\pi}{2}\eta\right] \cdot e^{i\omega t}. \tag{11}$$

The only unknown of this single degree of freedom system represented by Eq. (11) is the rotation amplitude at the base of the rocking cylinder $\bar{\Theta}$ under harmonic base excitation. This quantity is computed by considering moment equilibrium at the base of the cylinder (see Fig. 3) including the inertial terms:

$$M_b^0 - \bar{\Theta} M_b^1 - \frac{1}{2} M_g H \ddot{X}_g + I_y \omega^2 \bar{\Theta} = K_\theta \bar{\Theta}, \tag{12}$$

where M_b^0 is the moment amplitude induced by the pressures exerted by soil on a corresponding fixed-base cylinder, M_b^1 is the moment amplitude induced by the pressures associated with a unit rotation of the cylinder base, M_g is the mass of the cylinder, $I_y = M_g R^2/4 + M_g H^2/3$ is the mass moment of inertia of the cylinder with respect to an horizontal axis passing through the cylinder base. Inverting Eq. (12) the frequency-dependent, complex-valued rotation, may be computed from the following relation:

$$\bar{\Theta} = \frac{M_b^0 - M_g H \ddot{X}_g/2}{K_\theta - I_y \omega^2 + M_b^1}. \tag{13}$$

A fundamental aspect of the solution concerns the rotational impedance to be used to model the dynamic interaction between the base of the cylinder and the deformable half-space underneath. This problem was solved using the results obtained by Veletsos and Verbic [1974] in their study of a rigid, massless disk resting at a surface of a homogeneous, linearly elastic half space. The resulting rotational impedance is defined as $K_\theta = K_\theta^{st}(k_\theta + i a_{0b} c_\theta)$ where $K_\theta^{st} = 8GR^3/[3(1-\nu)]$ is the static stiffness, and k_θ and c_θ are functions of the dimensionless frequency $a_{0b} = \omega R/V_{sb}$ for a discrete set of values of Poisson's ratio $\nu = 0,\ 1/3,\ 0.45,\ 0.5$.

Selection of the rotational impedance derived by Veletsos and Verbic [1974] has been critically reviewed and compared with other approaches particularly in relation to the effects of disk embedment [Pais and Kausel, 1990]. The advantage of this approach has been confirmed also by other independent studies like for instance the model by Novak and Aboul-Ella [1978] on base reactions of piles. See Beltrami [2004] for more details on this issue.

It is noted that since the global impedance of the rigid cylinder is built as a sum of the horizontal layer impedance plus the rotational contribution of the base, the rocking-swaying coupling and the embedment effects are implicitly taken into account in the global moment equilibrium equation. The model has been implemented in a computer code and generalised for an arbitrary, transient input ground motion using the FFT technique. The core of the algorithm is the computation of the transfer functions representing the horizontal displacement and rotation at the top centre point of a rigid cylinder generated by a uniform, horizontal harmonic

excitation of unit amplitude applied at the bedrock-layer interface. Then the algorithm computes the natural modes of vibration of the stratum and the horizontal pressures exerted by the soil along the surface of the cylinder taking into account the rotational impedance of the base.

The transfer function is computed up to a maximum frequency f_{max} to limit the number of modes N_{max} that need to be considered in the analysis. The value of f_{max} has been set as the smaller of the Nyquist frequency associated with the seismic input (i.e. $f_{ny} = 1/(2dt)$ where dt is the sampling time of the accelerogram), and the frequency upper limit assumed for the linear-equivalent site response analysis ($\sim$25 Hz). The latter has been required to deconvolve the free-field seismic input recorded at the outcropping bedrock (see Fig. 7), to the base of the large-diameter shaft. It should be remarked however that in general f_{max} is a variable quantity as it depends upon the geometry and the properties of a given system. Going from stiff to soft soils and/or from short to long cylinders while keeping the same accuracy will require considering a larger number of modes.

3.1. *Extension of the model to "rough" and "smooth" interfaces*

The model described above is linear. The only way nonlinearity can somehow be accounted for is during the computing of the strain-compatible, dynamic parameters of soil (i.e. shear stiffness and material damping ratio). However at the top of the cylinder close to the free-surface, large deformations and thus nonlinear effects are expected to take place. In this zone in fact the overburden pressure is low and hence the shear strength at the foundation-soil interface is reduced. On the other hand large displacements and rotations are developed as a consequence of the position of the cylinder cap with respect to the rocking base.

These observations motivate the need to find a better representation of the interface conditions at the top ring of the foundation. One could for instance neglect the shear stress and take into account only the normal stress component. In order to do so it is necessary to change the boundary condition leading to Eq. (6) from "rough" (which corresponds to a perfectly welded interface), to "smooth" interface where the circumferential shear stress is assumed always equal to zero.

To solve this problem the constants of integration A, B and Δ of Eq. (6) for the impedance of the constrained BN layer must be recalculated using the "smooth" boundary condition. A simple computation yields [Beltrami, 2004]:

$$\begin{aligned} A &= -\frac{1}{\Delta}[4K_1(\lambda) + 2\lambda K_0(\lambda) + \lambda^2 K_1(\lambda)], \quad B = -\frac{1}{\Delta}[4K_1(\mu) + 2\mu K_0(\mu)], \\ \Delta &= [K_1(\mu) + \mu K_0(\mu) \cdot [3K_1(\lambda) + 2\lambda K_0(\lambda) + \lambda^2 K_1(\lambda)] \\ &\quad - K_1(\lambda)[3K_1(\mu) + \mu K_0(\mu)]. \end{aligned} \tag{14}$$

With these newly defined constants of integration, the BN layer impedance of a "smooth" interface may be computed by integrating the normal stress component

along the surface of the cylinder:

$$K_n = -\int_0^{2\pi} [\sigma(1)\cos(\theta)^2] R d\theta = -\pi R \sigma(1) = K_n^s. \tag{15}$$

The resulting stresses and forces at the soil-cylinder interface may be computed as for the case of a "rough" interface from the product of the layer impedance with the difference between the horizontal displacement computed in the far-field (shear beam model) and the cylinder centre axis.

It should be remarked that the normal stresses computed for the "smooth" and "rough" interfaces are in general different. Usually the normal stress associated with the "smooth" interface is greater than that relative to a "rough" interface as it is the only resisting component of the dynamic soil pressure.

The height $\mathrm{H} \cdot (1 - \eta_r)$ of the foundation top ring, that may be assumed with a "smooth" interface, can be computed from a preliminary analysis conducted with a uniform "rough" interface. From the results of this analysis one can easily establish the extension along the shaft of the "smooth" zone based on the exceedance of a prescribed threshold shear stress.

The most important implication of the existence of mixed (i.e. smooth and rough) interface conditions along the cylindrical foundation is on the magnitude of the kinematic internal forces. In fact a variation of the horizontal layer impedance along the height of the shaft leads to a discontinuity in the shear and moment diagrams at the change of interface type (see Beltrami [2004] and Beltrami *et al.* [2005] for more details).

3.2. *Extension of the model to inhomogeneous soil profiles*

Modelling soil inhomogeneity [Dobry *et al.*, 1976; Schreyer, 1977; Davis *et al.*, 1994] is of great importance in engineering practice since almost all soil deposits are characterised by some degree of vertical heterogeneity. An extension of the kinematic model illustrated in the previous sections to a vertically inhomogeneous soil stratum has been implemented by modifying the free vibration modes of the cantilever shear beam used to simulate the far-field response of the model.

The exact analytical solution of the free vibration problem (i.e. computation of natural frequencies and mode shapes) of an inhomogeneous layer has been derived by Pecker and Afra [1995] and Pecker [2003, 2004] for the case of a shear wave velocity profile varying as a power function of depth with an arbitrary exponent "p":

$$V(z) = V_S \left(\frac{z}{H}\right)^{\frac{p}{2}}, \tag{16}$$

where V_S is the shear wave velocity at depth H and "p" is a quantity that may assume any value greater than zero and smaller than 2. Typically, for coarse-grained geomaterials $p = 0.45$–0.6 whereas for normally consolidated clays $p = 0.8$–1 [Pecker

and Afra, 1995]. The natural frequencies of the stratum may be evaluated from the roots $\bar{\rho}_n$ of the following Bessel's function of the first kind of order $(p-1)/(2-p)$:

$$J_{\frac{p-1}{2-p}}(\bar{\rho}) = 0, \quad \text{from which } \omega_n = \bar{\rho}_n(2-p)\frac{V_S}{2H}, \tag{17, 18}$$

whereas the mode shapes, normalised to 1.0 at the free-surface are given by the following expression:

$$X_n(z) = [2/\bar{\rho}_n]^{\frac{p-1}{2-p}} \cdot \Gamma\left(\frac{1}{2-p}\right) \cdot (z/H)^{\frac{1-p}{2}} \cdot J_{\frac{p-1}{2-p}}\left(\bar{\rho}_n(z/H)^{\frac{2-p}{2}}\right), \tag{19}$$

where $\Gamma(\cdot)$ is the Gamma function. Besides a small increase in computational effort, if compared with the solution of a homogeneous layer, now the solution can no longer be obtained using the method of separation of variables, as the constraint layer stiffness k_n is at this time function of both ξ and η coordinates. However, as suggested by Veletsos and Younan [1994b] for the case of a rigid earth-retaining wall, a reasonable approximation to the solution may be obtained by computing the numbers k_n through the equation $k_n = \rho\omega_n^2$ which implicitly assume k_n to be constant. In this case the circular frequency ω_n represents the nth natural frequency of the inhomogeneous stratum vibrating as a cantilever shear beam. The approximation by Veletsos and Younan [1994b] exhibits the following two features:

- The evaluation of shear stresses acting on the upper and lower faces of the horizontal BN disk is exact for the free vibration of the nth natural mode $X_n(\eta)$;
- For the limiting case of a statically excited stratum the approximate solution is in good agreement with numerical solutions obtained using the finite element method.

Both features are retained also by the present cylindrical model.

With this approximation the extension of the model to an inhomogeneous soil stratum is obtained by using mode superposition with a depth-dependent, elastically constrained BN layer impedance. Veletsos and Younan [1994b] suggested that the soil layer impedance K_n may be dependent on the depth η only in the static term:

$$K_n(\eta) = [K_n(\eta)]_{st}(\alpha_n + i\phi_n\beta_n), \tag{20}$$

where α_n and β_n are frequency dependent stiffness and damping factors and $\phi_n = \omega/\omega_n$.

As for the case of a homogeneous soil stratum, the complex-valued, horizontal dynamic force per unit length of cylinder may be simply expressed by the product of the depth-dependent layer impedance $K(\eta)$ and the difference between the horizontal displacement computed at the far-field (shear beam model) and the cylinder centre axis.

For the rotational boundary condition at the base of the cylinder, knowing that the fundamental mode of vibration of the layer has a linear shape with the displacement increasing from the base to the top, the horizontal dynamic force

per unit length of cylinder may be written in a form similar to that suggested by Veletsos and Younan [1994b] for rigid walls, namely:

$$F(\eta, t) = \left[K_1(\eta)(U_1 - W_1)\eta + \sum_{n=2}^{N_{max}} K_n(\eta) U_n X_n(\eta) \right] \cdot e^{i\omega t}. \tag{21}$$

From the knowledge of the horizontal force distribution along the cylinder height, the resultant moments and shear forces can be easily obtained by numerical integration.

Finally it is remarked that the above results can be used to model different kinds of soil-foundation interfaces along the height of the cylinder from "*rough*" to "*smooth*", as the theory illustrated in Sec. 3.1 remains applicable also to the case of a inhomogeneous soil stratum.

3.3. *Characteristics of the model under "static" harmonic excitation*

This section will illustrate the "static" distribution of normal (radial) and tangential circumferential stresses induced by the soil surrounding the cylinder at the foundation soil-interface. It should be remarked that the word "static" here is used with a meaning of a harmonic excitation having a frequency of oscillation $\omega = 0$. The excitation is applied in the direction of the X-axis (see Fig. 3). The so-called "static" limit of a dynamical system, which in this case is constituted by a cylinder subjected to a system of forces representing the soil reactions to a seismic excitation, is an important characteristic and is often difficult to obtain with an acceptable level of accuracy.

Figure 4 shows the distribution of the lateral "static" normal and tangential stresses obtained from the model described above applied to a 15 m thick, homogeneous layer characterised by a shear wave velocity $V_S = 150\,\mathrm{m/s}$. The soil-foundation interface along the length of the shaft is assumed "rough". From the coloured-stress map it is evident that the magnitude of normal and shear stress is distributed along the shaft with an opposite pattern: At locations where the shear stress reaches relatively high values, the normal stress is low and vice versa. This is not surprising as the equations for normal and tangential stresses are dependent respectively upon the cosine and sine of the circumferential angle θ as shown by the following relations:

$$\sigma_r = \sigma(\xi)\cos(\theta)e^{i\omega t}, \quad \tau_{r\theta} = \tau(\xi)\sin(\theta)e^{i\omega t}. \tag{22}$$

Since sine and cosine are orthogonal functions (i.e. they are 90° out of phase), the magnitude distribution of normal and shear stresses is opposite. Figure 5 shows the stress distribution under "static" conditions obtained from the model for different values of height and shear wave velocity of the homogeneous layer. From this figure it is possible to observe that in soft soils (or for short foundation shafts) the stress distribution is characterised by a regular, parabolic shape having a peak value

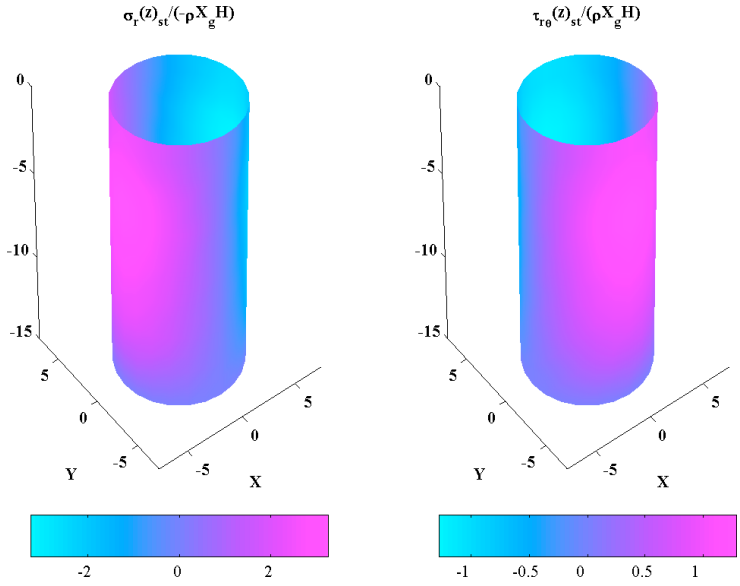

Fig. 4. Distribution of lateral "static" normal (left) and tangential (right) stresses for $H = 15\,\text{m}$ and $V_s = 150\,\text{m/s}$.

located near the mid height of the foundation. On the contrary, in stiff soils (or for long foundation shafts) the stress distribution ceases to be "regular" as it shows a sign inversion at a distance close to the top ring of the cylinder cap. This pattern of stress distribution is confirmed by Veletsos and Younan [1994b] for the case of rigid earth-retaining walls. It is also confirmed by the results of dynamic numerical simulations conducted with the finite-element method by Wood [1973] on a rigid earth-retaining structure that may rotate at the base; this solution is regarded in the literature as a sort of "exact" solution.

Figure 6 shows the "static" distribution of shear and moments internal actions along a 25 m long shaft, normalised to the static value at the base, and for different values of shear wave velocity of the homogeneous layer. The moment profile has a tendency to exhibit smaller values as V_S decreases (i.e. as the soil stratum gets softer). The shear profile displays a similar trend but with a more irregular pattern.

4. Validation of the Model with a Finite Element Code

The analytical, kinematic interaction model for large-diameter shaft foundations has been validated through a benchmark test conducted with the finite element code SASSI [1999].

This program is one of the most widely used computer software for solving soil-foundation-structure interaction problems. Data and geometry used for the benchmark test are illustrated in Fig. 7. The soil stratum has been modelled as a

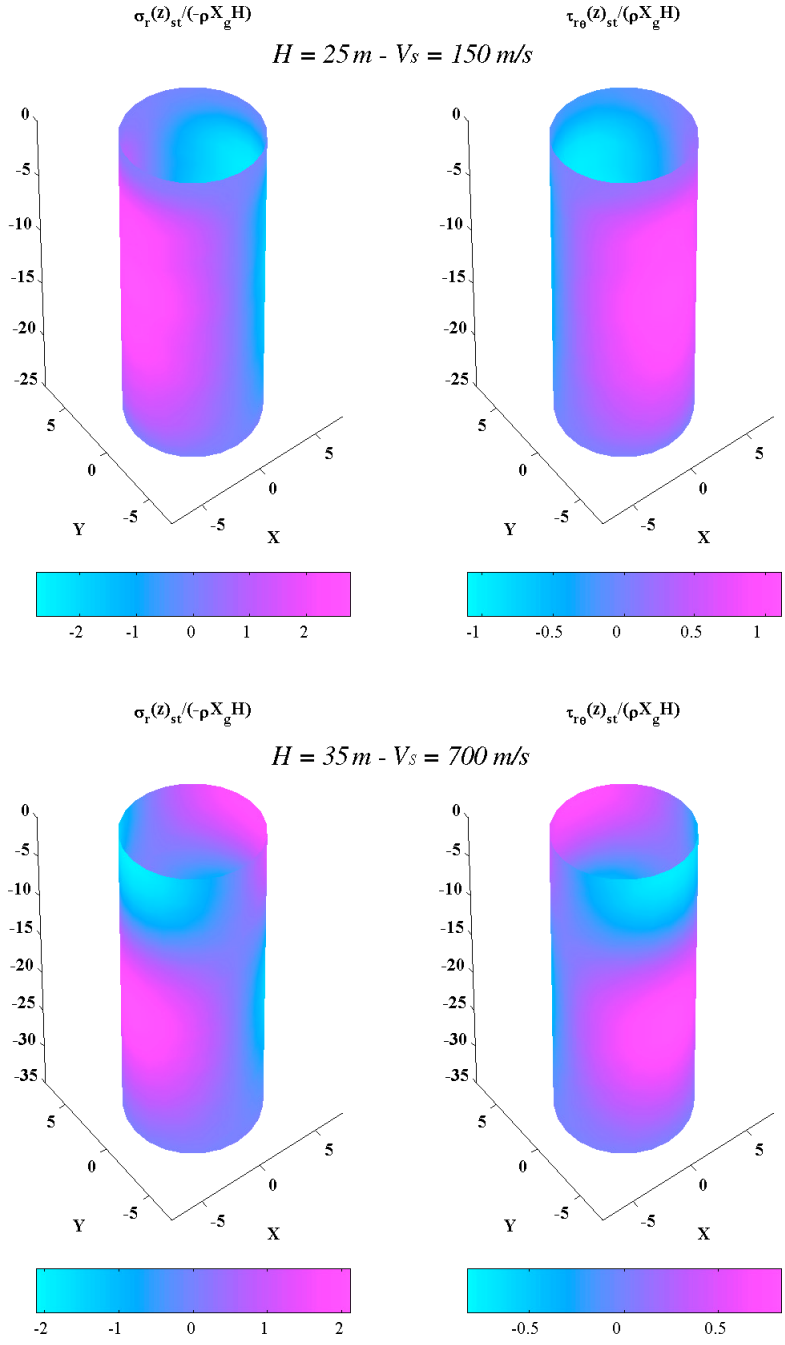

Fig. 5. Distribution of lateral "static" normal (left) and tangential (right) stresses for different height and shear wave velocity of the homogeneous layer.

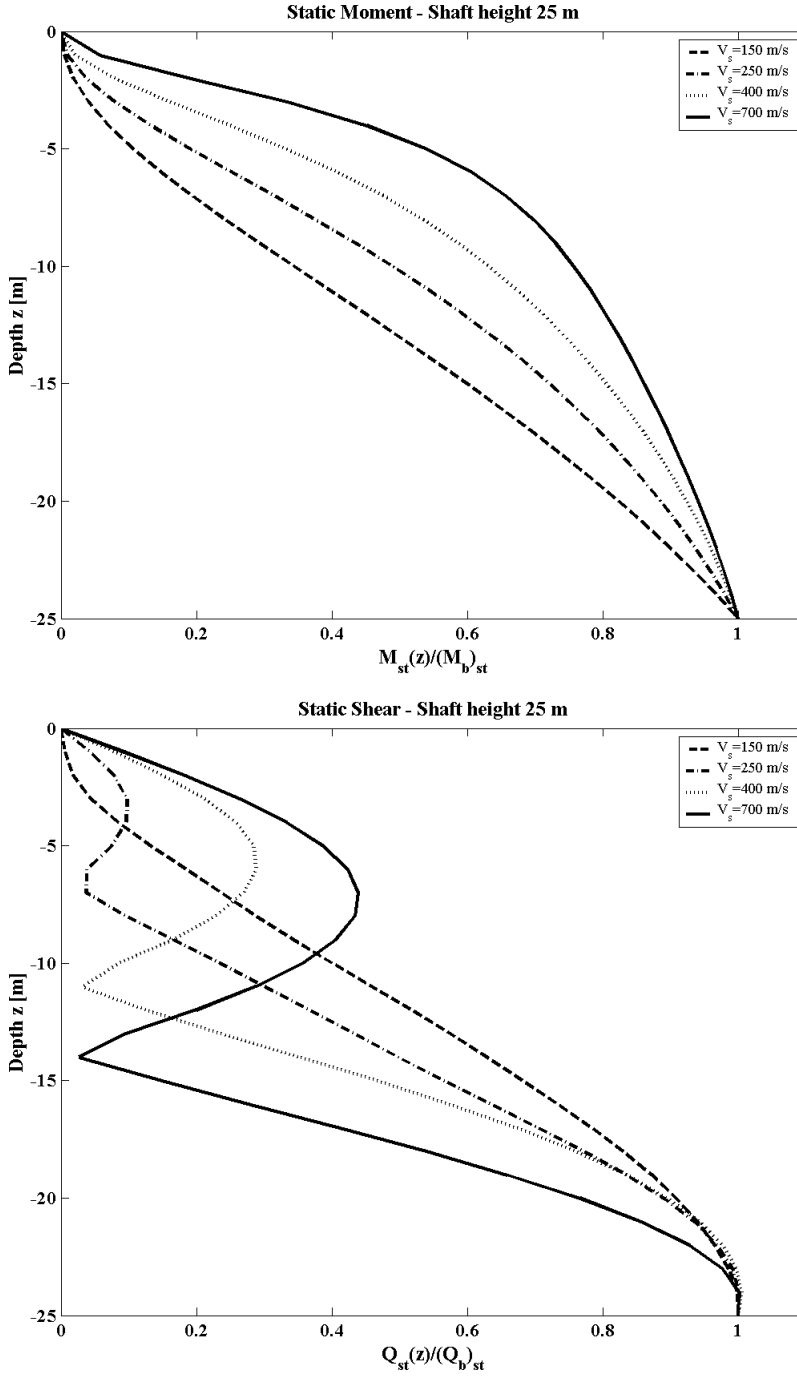

Fig. 6. Distribution of lateral "static" moment (top) and shear (bottom) for various shear wave velocity of the homogeneous soil stratum.

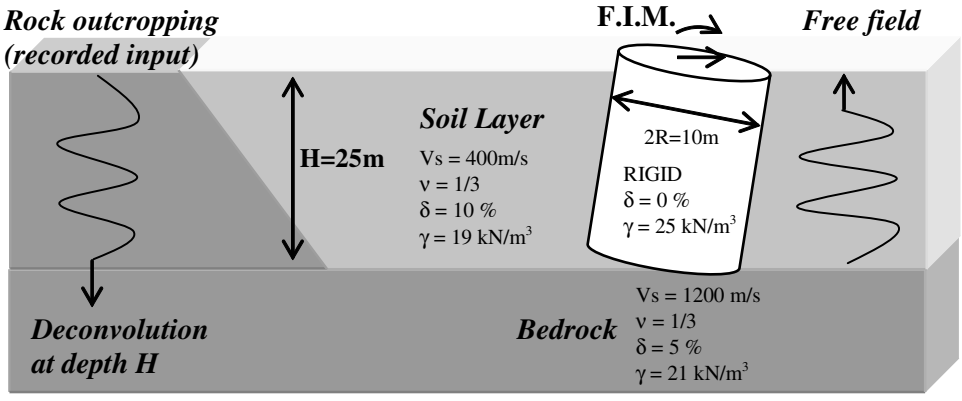

Fig. 7. Geometry and data of the problem solved by SASSI and the present model in the validation test.

homogeneous, semi-infinite, viscoelastic continuum placed on top of a viscoelastic half-space.

The solution is carried out using the substructuring approach.

The cylindrical shaft foundation is modelled using standard three-dimensional solid elements. The excitation is represented by a single horizontal component of an accelerogram prescribed at the free-field, outcropping rock (see Fig. 7).

The problem consists of determining the translational and rotational acceleration time-histories at the top of the foundation shaft. This corresponds to the so-called Foundation Input Motion (FIM) as shown in Fig. 7. From the acceleration time-histories of the foundation cap one can easily determine other types of response functions like the displacement or velocity time histories or the acceleration response spectra. The soil-foundation interface conditions throughout the surface of the shaft are assumed "rough".

The solution to the benchmark problem obtained with SASSI is compared with the results determined using the kinematic interaction model illustrated in the previous sections.

The ground motion selected at the outcropping rock for the validation test was the North-South component of the El Centro 1940 earthquake record which is characterised by a peak ground acceleration of $0.32\,g$. Both the analysis carried out with SASSI and that performed using the kinematic interaction model have been accomplished using a frequency cut-off of 25 Hz which consequently represents the highest frequency resolved in the analyses. Figures 8 and 9 illustrate the comparison of the results obtained from the validation test for the Foundation Input Motion (FIM). They are represented in terms of acceleration time histories, both translational and rotational, and the corresponding acceleration response spectra.

In general, the results obtained for the FIM computed with the proposed kinematic model are in good agreement with those determined with SASSI for both the acceleration time-histories and the acceleration response spectra. In Fig. 8 the

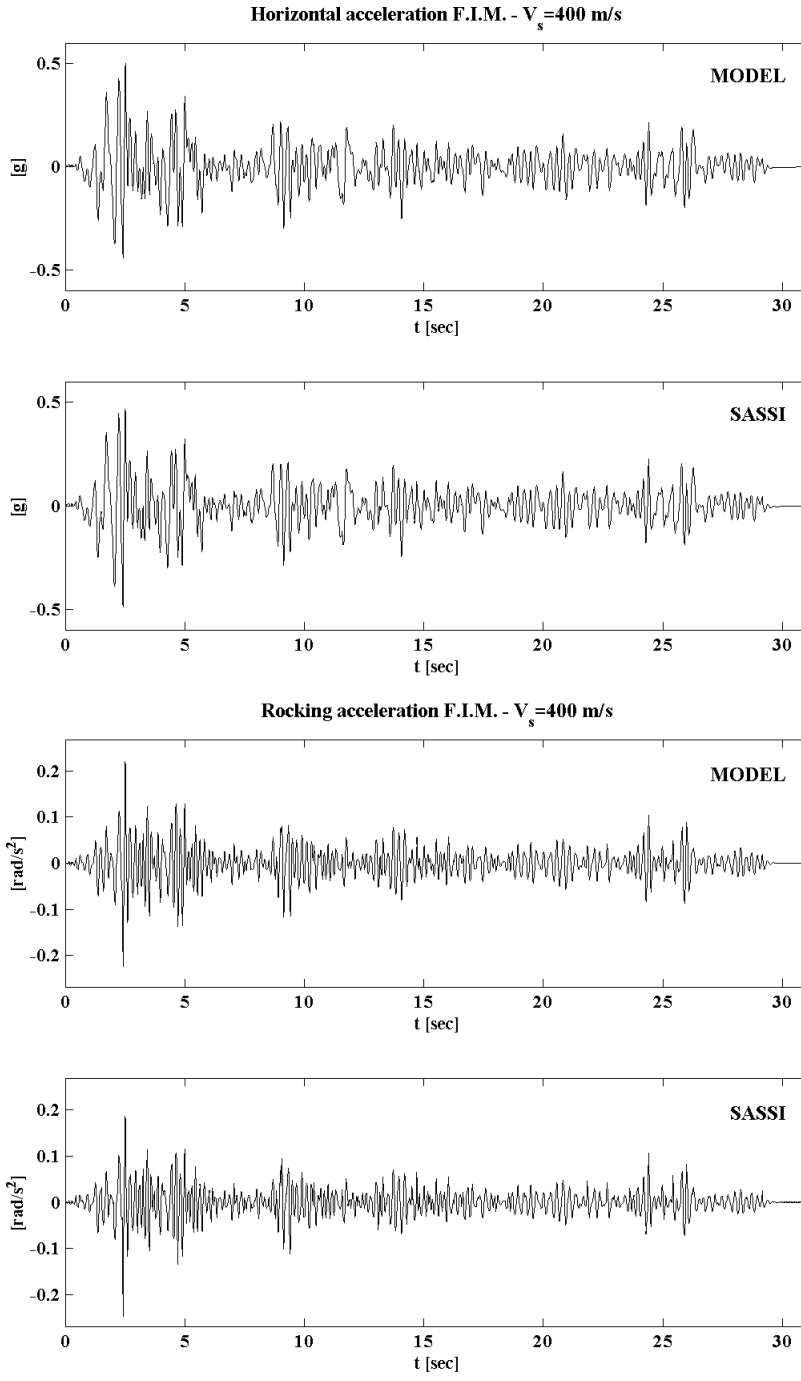

Fig. 8. Translational and rotational acceleration time-histories at the foundation cap (i.e. FIM) obtained with the finite element code SASSI and the kinematic interaction model for the benchmark test shown in Fig. 7.

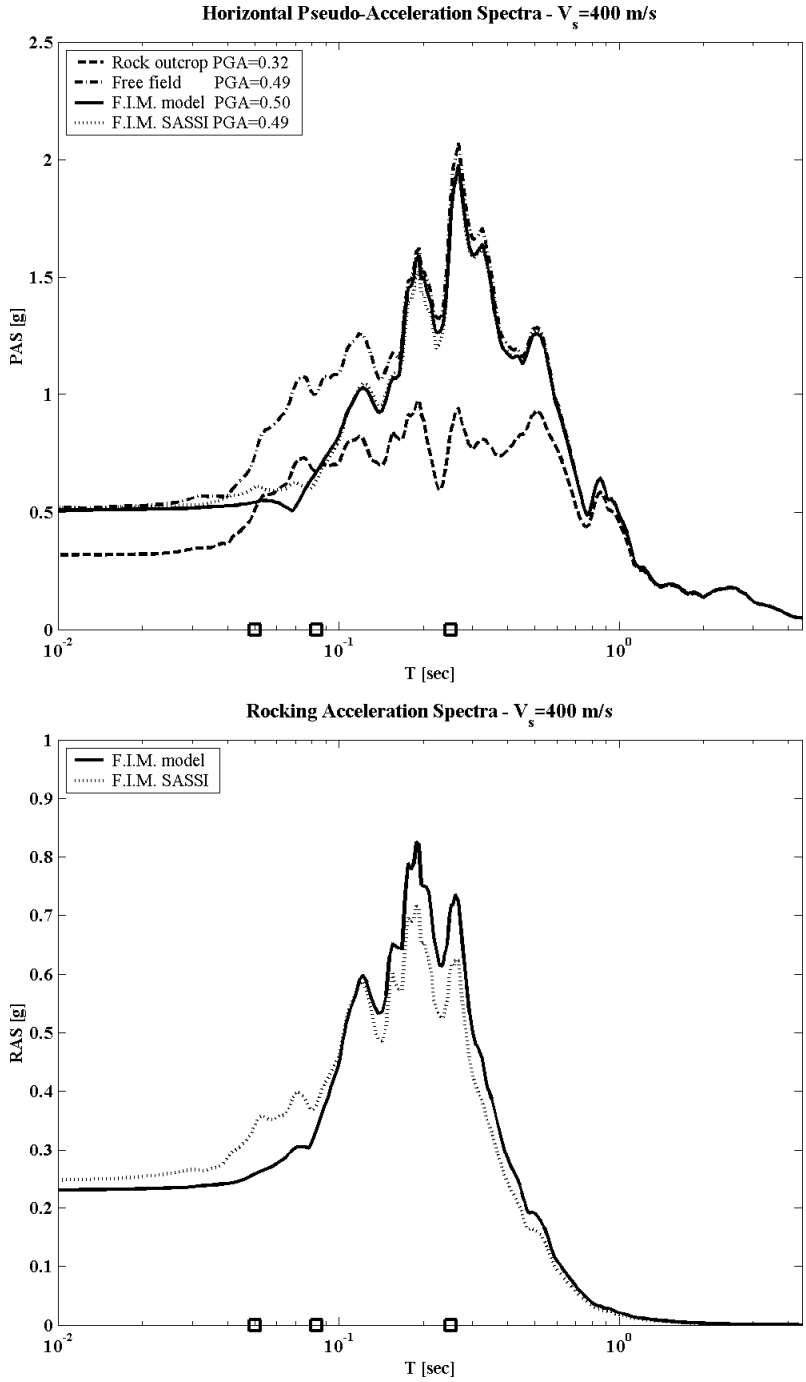

Fig. 9. Translational and rotational acceleration response spectra at the foundation cap (i.e. FIM) obtained with the finite element code SASSI and the kinematic interaction model for the benchmark test shown in Fig. 7. The symbol '□' represents the natural periods used in the analysis of the model by modal superposition.

time-histories computed with two approaches are very similar to each other, both in amplitudes and phases.

In Fig. 9 the horizontal acceleration response spectra computed with the kinematic model matches fairly well the spectra computed with SASSI in all period range. Both spectra show higher values of the ordinates at lower periods when compared with the free-field response. The rotational acceleration response spectra are also in good agreement even though the spectrum computed with the proposed kinematic model tends to slightly overestimate the response for $T > T_1$ (where T_1 is the fundamental period of vibration of the system) and moderately underestimate the response for $T < T_1$.

A similar agreement in the results is found for the solution of a problem identical to that illustrated in Fig. 7 but considering a stiffer soil layer (i.e. $V_S = 700\,\mathrm{m/s}$). For more details on the results obtained from this benchmark test the interested reader is referred to the work of Beltrami [2004].

5. Parametric Analyses of Kinematic Interaction Model in Homogeneous Soils

After the validation, it is now interesting to use the proposed model to throw light onto the phenomenon of kinematic interaction of large-diameter shaft foundations. For this purpose a comprehensive parametric study has been carried out to investigate the influence of foundation's length and layer's shear stiffness in the computed FIM. Table 1 illustrates the set of geotechnical parameters considered in this study for the soil system. The values assumed for the shear wave velocity of the layer are those of EC 8 [2003] Part 1 soil categories and cover a fairly wide range of geomaterials ranging from soft to very stiff soils. For the bedrock the value of V_S has been assumed constant.

Concerning the length of the shaft, three different slenderness ratios H/2R were considered covering typical values for this type of large-diameter foundations. With a constant radius $R = 5\,\mathrm{m}$, three lengths $H = 15 - 25 - 35\,\mathrm{m}$ were assumed. The variation in shear wave velocity of the stratum (four values of V_S ranging from 150 to 700 m/s) and the three different lengths H of the foundation yields a wide range of the layer fundamental period $T_1 = 4H/V_s$, ranging from 0.09 sec to 0.93 sec. The mechanical impedance ratio $\rho_S V_S/\rho_B V_{SB}$ at the soil layer/bedrock interface (see Table 1) varies from 0.53 to 0.11.

Table 1. Geotechnical properties assumed in the parametric study for the soil system.

Soil class according to EC8		B		C	D	A(*)
Shear wave velocity [m/s]	V_s	700	400	250	150	1200
Poisson ratio	ν	1/3	1/3	1/3	1/3	1/3
Damping [%]	$\delta = 2 \times D$	10	10	10	10	5
Specific weight [kN/m^3]	γ		19			21

(*) bedrock

Figures 10 and 11 show the results of the kinematic interaction analysis of the large-diameter shaft using the model illustrated in Sec. 3 for an homogeneous stratum and a "rough" interface. The seismic excitation selected at the outcropping rock for the numerical simulations was the East-West component of Duzce accelerograms recorded during the 12/11/1999 Turkey earthquake. These data were retrieved from the PEER [2004] strong motion database, and correspond to an earthquake scenario of moment magnitude $M_w = 7$ and closest distance to the fault rupture of 30 km.

The Duzce accelerogram has been adjusted for spectral compatibility with the response spectrum obtained for the same earthquake scenario using the Abrahamson and Silva [1997] attenuation relationship, characterised by a PGA $= 0.20\,g$. The spectral matching, up to the first natural period of the soil-foundation-structural system, has been performed in the time domain using the "*time-history adjustment method*" [Kaul, 1978; Lilhanand and Tseng, 1988; Abrahamson, 1992]. The interested reader is referred to [Beltrami, 2004] for more details on the application of this technique for spectral matching of an original ground motion accelerogram.

Figures 10 and 11 clearly show that for large-diameter shaft foundations the effects of wave scattering originated by kinematic interaction is important and the difference between the motion computed at the foundation cap and the free-field ground motion may be very significant, particularly in soft soil layers. However the most important aspect, is that kinematic interaction is responsible for inducing a rocking excitation at the top of the shaft even if the free-field ground motion is solely composed by a horizontal excitation. This has important consequences in the seismic response of a structure founded on large-diameter, deep pile foundations as will be demonstrated in the next section.

The complete set of results of the parametric study including the time-histories of FIM is reported in [Beltrami, 2004] and is not included here due to limitations in paper length. From this report, the horizontal component of the acceleration calculated in soft soils (i.e. for $V_S = 150$–250 m/s) at the top of the foundation shaft, is considerably lower than the free-field ground motion, although the two records have the same phases. Furthermore as expected, in stiff soil layers (i.e. for $V_S = 400$–700 m/s), FIM is characterised by a higher frequency content if compared with FIM of softer soils. The opposite is true for the low frequency content of the response.

The reduced FIM response in soft soils with respect to the free-field ground motion observed for the horizontal acceleration holds also, though to a lesser extent, for the velocity time histories. For the displacement response the difference between free-field and FIM excitation is almost negligible. The difference between FIM and free-field ground motion caused by kinematic interaction increases as the wavelength of seismic (shear) waves decreases to become smaller than the size of the foundation. For the same frequency of excitation and foundation size this phenomenon is expected to be more pronounced in soft soils.

These observations inferred from the seismic response of the soil-foundation system in the time domain get also reflected in the response spectra. From Fig. 10

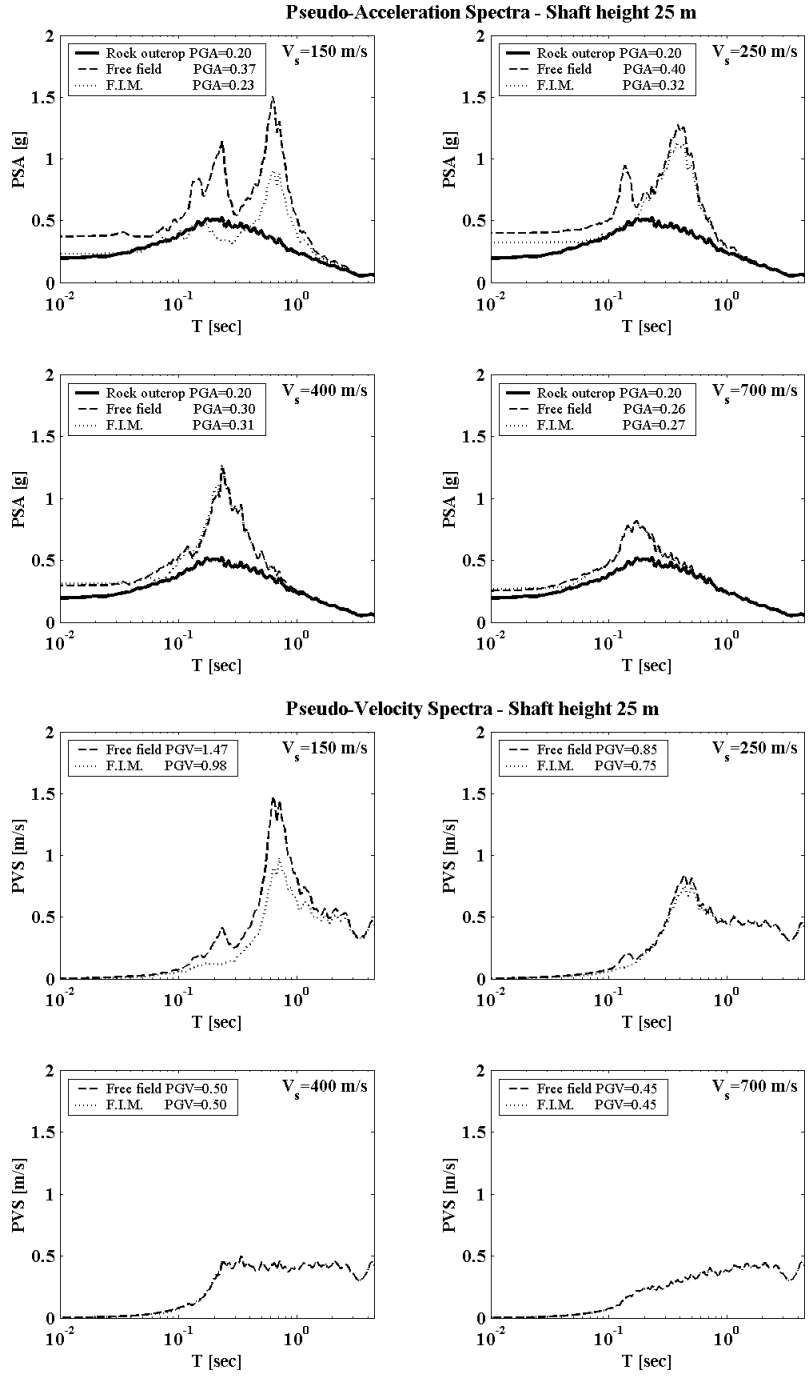

Fig. 9. Comparison of free-field and FIM horizontal acceleration and velocity response-spectra obtained using the proposed kinematic interaction model.

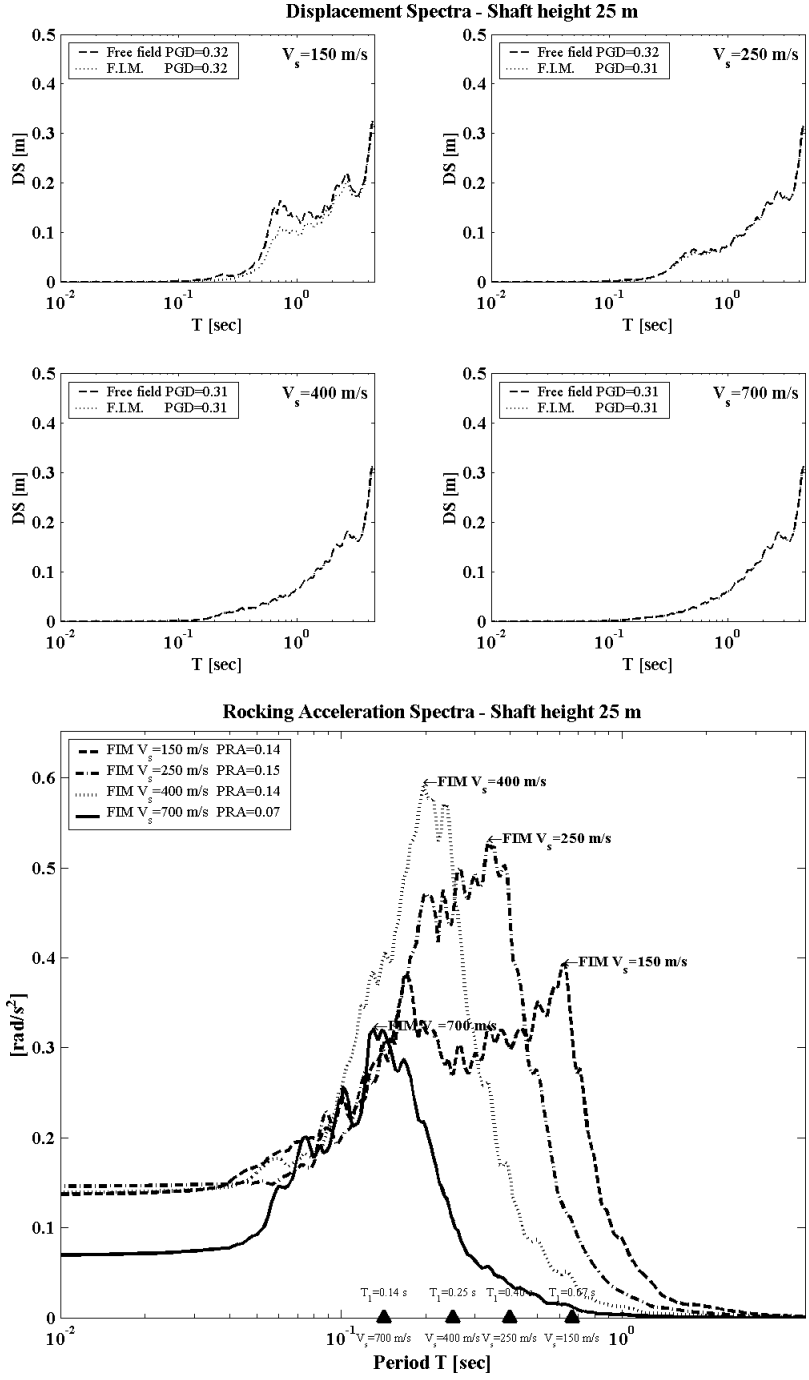

Fig. 10. Comparison of free-field and FIM horizontal displacement and rotational acceleration response-spectra obtained using the proposed kinematic interaction model.

(top four figures) in fact it can be noticed that in the short period range, the spectral ordinates of FIM horizontal acceleration response spectra are noticeably lower than the free-field response and this effect is more pronounced in soft soils (i.e. for $V_S = 150$–$250\,\mathrm{m/s}$). As a limit case, the zero-period intercept of FIM response spectrum (representing the Peak Ground Acceleration or PGA) for $V_S = 150\,\mathrm{m/s}$ approaches the PGA $= 0.20\,g$ of the outcropping rock which is 85% lower than the PGA of free-field ground motion (i.e. at the free-surface of the soil layer).

Another observation suggested by Fig. 10 (top four figures) is that whereas in soft soils the free-field response exhibits two peaks in correspondence to the first two natural periods of the layer, the FIM acceleration response spectrum amplifies only the first period as the peak corresponding to the second period is strongly damped. Physically what is happening is that under the earthquake loading the foundation (which is assumed rigid) is able to comply and thus amplify mainly the first mode only of the soil layer whose shape is one quarter of a sinusoid from the base layer to the top. On the contrary the large-diameter shaft is almost totally unaffected by the layer second mode whose shape (a portion of a sinusoid with a displacement change of sign) cannot be matched by the displacement of a rigid cylinder. The end result of this "*kinematic interaction*" is that the amplification of the second mode is *filtered-out* and the energy associated with it is not transmitted to the superstructure. As it always happens, this process of filtering the second and higher modes of vibration of the soil layer, is not completely "*free of charge*" for it is accompanied by a *side-effect* which is the rotational motion of the top of foundation shaft.

Concerning stiffer soil layers Fig. 10 (top four figures) shows (e.g. $V_S = 700\,\mathrm{m/s}$) that at low periods the spectral ordinates of FIM horizontal acceleration response spectra approximately match those of the free-field ground motion with a PGA that is almost the same for the two cases. The horizontal velocity response spectra (see Fig. 10 bottom four figures) display similar features. In particular in soft soils (e.g. $V_S = 150\,\mathrm{m/s}$) the FIM response is attenuated with respect to that of the free-field. On the contrary, the horizontal displacement response spectra of FIM and free-field ground motion illustrated in Fig. 11 (top four figures) are almost identical for both soft and stiff soils because, as mentioned above, the displacement response of the system is not affected by high frequencies.

Among all the features illustrated in this parametric study, the one with the most significant implications is certainly the "*conversion*" operated by the soil-foundation system of a purely translational (horizontal) excitation prescribed at the outcropping rock into a *coupled*, *swaying-rocking* excitation at the top of a rigid-piled foundation. Two mechanisms cause this "*kinematic conversion*" of the excitation: The first is due to the rotational deformability of the bedrock at the basis of the rigid cylindrical foundation; the second mechanism is related to dynamic pressures exerted by the soil surrounding the foundation which in general have a resultant that do not coincide with the centre of gravity of the large-diameter

shaft. As mentioned above, this mechanism is strongly linked to the wavelength of the propagating seismic (shear) waves and to the *filtering effect* operated by the rigid-body movement of the foundation onto higher modes of vibration of the soil layer.

Figure 11 (bottom figure) shows the FIM rotational acceleration response-spectra obtained using the proposed kinematic interaction model for the four values of V_S considered in this study (see Table 1) and for a foundation height $H = 25\,\text{m}$. It can be noticed from the figure that amplification of rocking motion occurs only at periods lower than the first natural period $T_S = 4H/V_S$ of soil layer[‡] and it is mostly concentrated around T_S. The peak rotational acceleration tends to exhibit higher values as the (shear) stiffness of the soil layer increases, although this interpretation does not hold for $V_S = 700\,\text{m/s}$.

6. Application of the Kinematic Interaction Model to Seismic Demand Assessment of a Bridge

The kinematic interaction model described in the previous sections has been applied to evaluate the seismic demand of a viaduct founded on large diameter shafts. Figure 12 shows the longitudinal view of the bridge of balanced cantilever girder type forming a continuous segmental prestressed concrete deck of 110 m spans. The bridge is symmetrical with respect to the central mid-span and crosses a wide valley characterised by the presence of a soft top soil stratum of variable thickness overlaying the bedrock.

The piers have heights of 75 m, 50 m to 30 m; they are connected with large-diameter shaft foundations passing through the soil layer and founded on the top of the bedrock roof. The soft soil layer has a variable thickness along the bridge to simulate a realistic alluvial, laterally inhomogeneous soil deposit. Furthermore, it is characterised by different values of shear wave velocity V_S (see Table 1) to cover the whole range from soft to stiff soil categories reported in EC8 [2003].

The dynamic response of the bridge will be used to study the effects of seismic Soil-Foundation-Structure Interaction (SFSI) by means of the substructuring approach which assumes the validity of the superposition theorem. Primary focus of the study will be to throw light into the phenomenon of kinematic interaction and of its implications for the seismic response of a structure investigating the influence of parameters such as foundation geometry and soil (shear) stiffness. Due to the symmetry of the bridge only piers P1, P2 and P3 will be analysed (see Fig. 12).

A linear, dynamic transient analysis of the bridge has been carried out using the finite element program ADINA [2003]. The Foundation Input Motion (i.e. FIM) has been computed using the kinematic interaction model for large-diameter shafts described in the previous sections. The seismic excitation at the outcropping rock

[‡]T_S is approximately equal to 0.67; 0.40; 0.25 and 0.14 seconds for $V_S = 150$; 250; 400 and 700 m/s respectively.

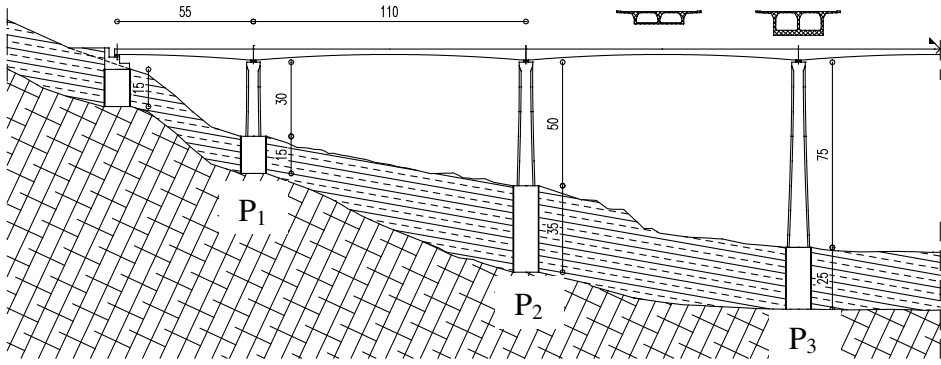

Fig. 11. Longitudinal view of the viaduct used to study soil-foundation-structure interaction and longitudinal section of the foundation subsoil.

is defined by the East-West and North-South components of Duzce accelerograms recorded during the 12/11/1999 Turkey earthquake and adjusted for spectral compatibility according to the procedure described in the previous section. The two accelerograms have been considered to act simultaneously.

The effects of soil deformability and energy dissipation occurring in the soil surrounding the foundations have been evaluated through a set of complex-valued, frequency-dependent, dynamic impedance functions computed for all degrees of freedom of the nodes at the base of the piers using the computer code DYNA4 [Novak M. *et al.*, 1994]. The response of the viaduct to earthquake loading has been assessed for the four soil categories reported in Table 1 and corresponding to those reported in Eurocode 8 Part 1 [EC8, 2003].

The main objective of this study is to evaluate the importance of the contribution of coupled swaying-rocking FIM excitation in the seismic demand assessment of the bridge. This is carried out through a comparison of the internal actions (i.e. axial and shear forces, bending and torsional moments) at the base of the piers computed for these two sets of excitations:

- FIM considering only the translational (horizontal) component of motion;
- FIM considering the coupled swaying-rocking components of motion.

The modal analysis of the viaduct yielded interesting results. The first natural period of the structure considered fixed at the base of each pier, is equal to $T_1 = 2.4$ seconds. The expected increase in T_1 resulting from the soil deformability is almost negligible ($T_1 = 2.5\,\text{sec}$). This happens because the large-diameter shaft foundation with the surrounding soil forms a relatively rigid system that restrains the deformability of the structure at its base as if the bridge foundations were clamped.

The first natural mode shapes of the structure are those of a continuous beam on elastic supports. In particular the fundamental mode shows each span of the bridge displaced in the typical single-wave bending shape whereas the second mode

is characterized by a double-wave bending shape with nodes at mid-span of the viaduct.

6.1. *Computation of base pier seismic demand*

Figures 13 through 15 illustrate the internal actions at the base of each pier obtained from the linear, dynamic, transient analysis of the bridge. They have been computed for each of the four values of shear wave velocity V_S that have been considered for the soil layer surrounding the foundation shafts (see Fig. 12 and Table 1).

The figures show that in all cases the effect induced by coupled swaying-rocking excitation is to increase the seismic demand of the piers in terms of both bending and torsional moments, and shear and axial forces.

However there is a difference in the increment of seismic demand between soft and stiff soil layers. Whereas in soft soils the rocking excitation is responsible for an increase of shear and moment seismic demand at the base of the piers (whose height is 35, 50 and 75 m) that reaches up to + 20% in the transverse direction, in stiff soils this rocking effect is negligible.

By comparing Figs. 14 and 15 the base longitudinal and transversal internal actions it is easy to observe that the increment in seismic demand is more pronounced for the longitudinal components which is the direction where the piers are more constrained and the structure behaves as a frame. These frame actions induce a large increase of longitudinal base moment demand (since it is nearly proportional to rotation times $3EJ/H$) that can reach up to + 40% in the tallest piers. The longitudinal base shear action is also incremented even though to a smaller percentage (since it is nearly proportional to rotation times $3EJ/H^2$).

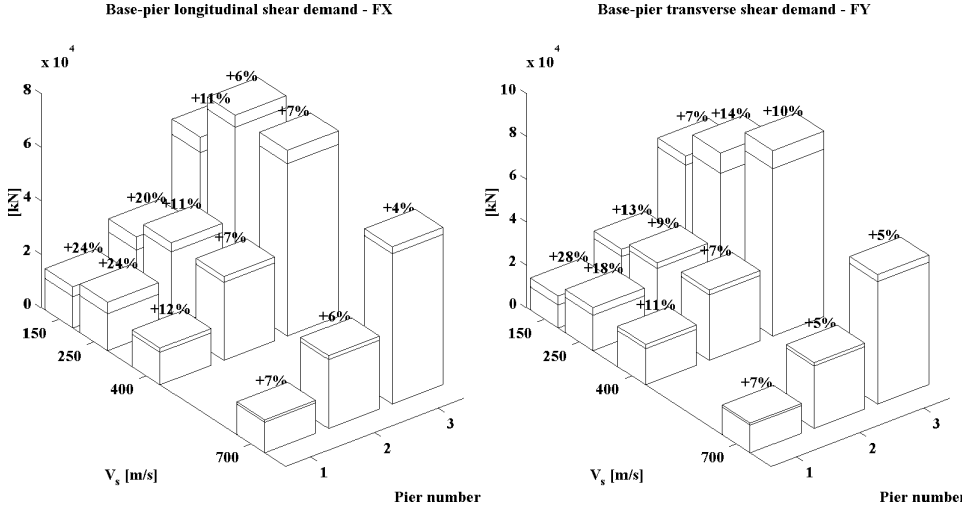

Fig. 12. Longitudinal (FX) and transverse (FY) base-pier shear demand: The percentages shown indicate the increment induced by coupled swaying-rocking excitation.

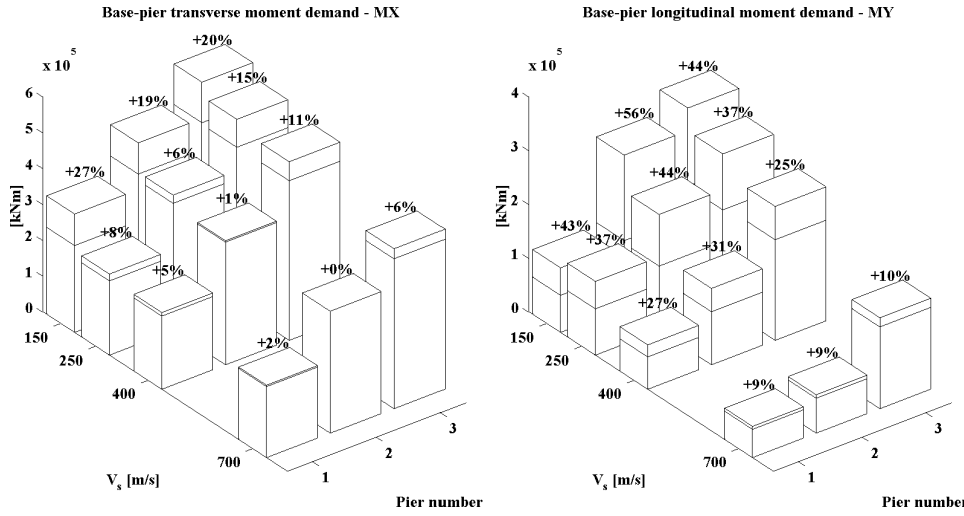

Fig. 13. Transverse (MX) and longitudinal (MY) base-pier moment demand: The percentages shown indicate the increment induced by coupled swaying-rocking excitation.

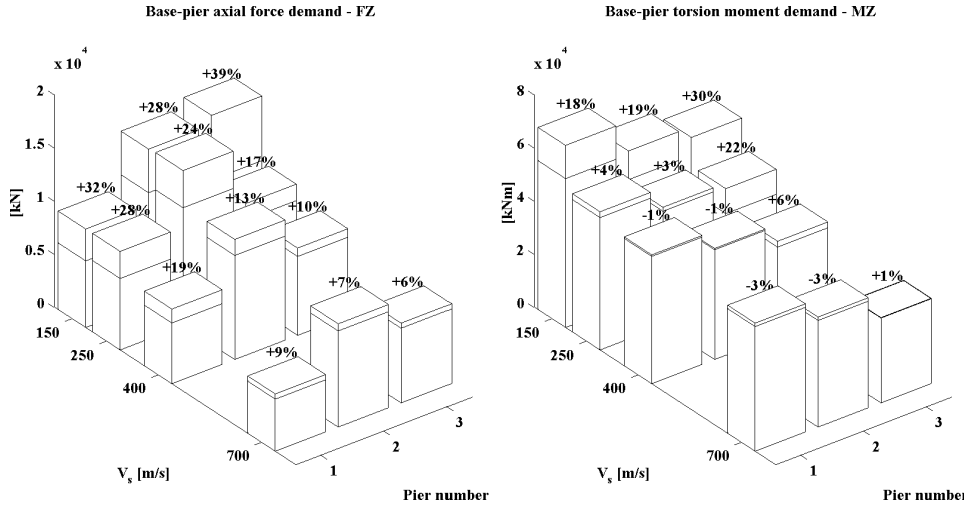

Fig. 14. Axial force (FZ) and torsion (MZ) base-pier demand: The percentages shown indicate the increment induced by coupled swaying-rocking excitation.

Figure 15 also shows this "frame effect" in terms increase of axial load and torsional moment at the base of each pier that in the softer soil layer may reach up to + 30%.

An increment of about 10–20% in seismic demand on a structure due to the presence of rocking FIM excitation has already been recognized in the literature [see for instance Elsabee and Morray, 1977; EC8, 2003] and it should be emphasised however that the importance of this effect is intimately linked to the degree of connection of

the soil-foundation system with the superstructure since the frame geometry may play a crucial role in mobilizing rotational stiffness and hence moments capacity at the base-piers.

Furthermore it should be remarked that the effects imposed on the superstructure by the swaying-rocking FIM excitation must be distinguished by the so-called "isolation effect" produced by rocking of the bridge foundation. In fact whereas the latter is caused by the inertial forces arising in the superstructure, the former represents an active excitation generated by the kinematics of the soil-foundation system (in the example above constituted by large-diameter shaft-foundations).

6.2. *Foundation seismic demand and capacity*

The global, static bearing capacity of large-diameter piled foundations is in general very large. However full mobilisation of this capacity requires foundation settlements that may not be compatible with the compliance characteristics of the superstructure. As a result, the design of this type of foundation is generally governed by the serviceability limit state rather than its ultimate capacity. Although this reasoning has been conducted with reference to statics, its validity can also be extended to dynamics and it constitutes the rationale for the adoption of a linear model in the seismic analysis of large-diameter piled foundations.

For these foundations, the total seismic forces acting along the shafts are computed from the superposition of the effects caused by both kinematic and inertial interaction. These forces represent the global seismic demand placed on the foundations but also the minimum seismic capacity these foundations need to guarantee for a safe seismic design.

An important aspect in computing the seismic capacity of large-diameter shafts is related to the assumption made at the soil-foundation interface with regards to stress and displacement continuity. The kinematic model illustrated in the previous sections and its capabilities to simulate mixed "smooth" and "rough" boundary conditions at the soil-foundation interface allows a realistic computation to be made of seismic bearing capacity of the viaduct's shaft. Besides the dynamic component, the normal pressures exerted by soil along the surface of the pile includes also the static component which is represented by the horizontal, effective, lithostatic stress $\sigma'_{h0}(z) = K_0\sigma'_{v0}(z)$ where K_0 and $\sigma'_{v0}(z)$ are respectively the *at-rest* coefficient of soil pressure and the vertical, effective overburden pressure. Both $\sigma'_{v0}(z)$ and $\sigma'_{h0}(z)$ are function of depth z. The *at-rest* and not the *active* soil state has been considered to govern the static horizontal pressures because of the reduced displacement capacity of the foundation.

The shear capacity at the soil foundation interface has been evaluated to a first approximation using the static approach $\tau_{\lim}(z) = \sigma'_{h0}(z)\tan(\delta')$, where $\delta' = 2\phi'/3$ is the friction angle at the soil-foundation interface and ϕ' is the (peak) angle of shear resistance of soil. The seismic soil-foundation interface capacity has been computed by integrating the time-histories of dynamic soil pressures along the

surface of the shaft. During the calculation, both the normal pressure (in magnitude and sign) and the maximum local shear circumferential stress (that might exceed the interface shear resistance) are constantly monitored to ensure the correctness of the computed interface capacity along the surface of the shaft.

6.3. *Results for foundation seismic demand*

Figures 16 and 17 illustrate the envelope profiles of bending moment and shear internal actions along a 25 m long shaft for the four categories of soil layers reported in Table 1. The contributions of kinematic and inertial interaction have been plotted separately in the figure. The importance of kinematic interaction and thus of FIM rocking excitation is apparent in computing the total seismic demand (for both moment and shear) along the cylindrical foundation, particularly in soft soil layers. The contribution of inertial interaction is more difficult to interpret as it varies irregularly with soil stiffness.

An important general consideration that can be drawn from Figs. 16 and 17 is that the seismic behaviour of large-diameter piled foundations is governed in equal proportions by inertial and kinematic interaction effects and that neglecting the contribution of kinematic interaction would lead to a strong underestimation of the foundation seismic demand.

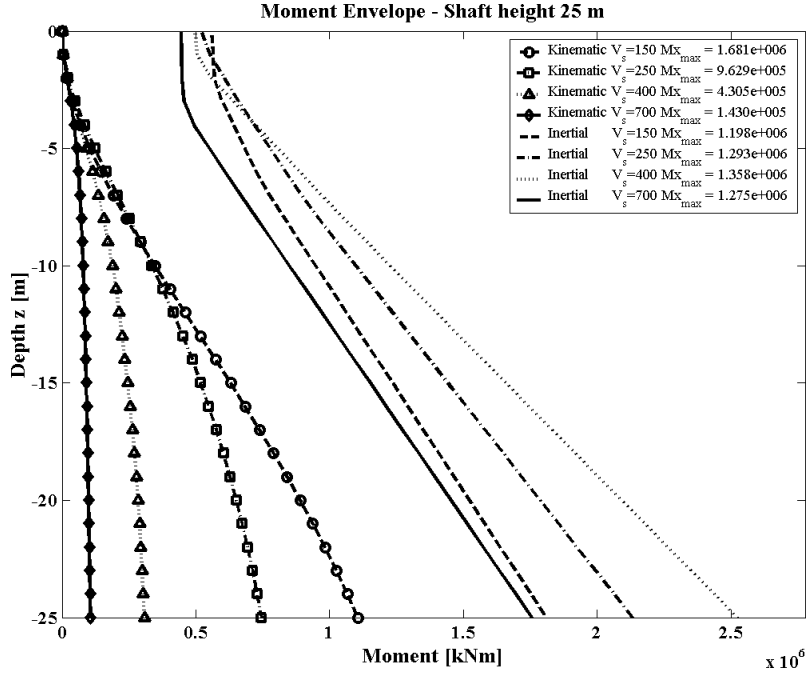

Fig. 15. Bending moment envelope profiles along a 25 m long shaft for the four categories of soil layers reported in Table 1. The contributions of kinematic and inertial interaction have been uncoupled.

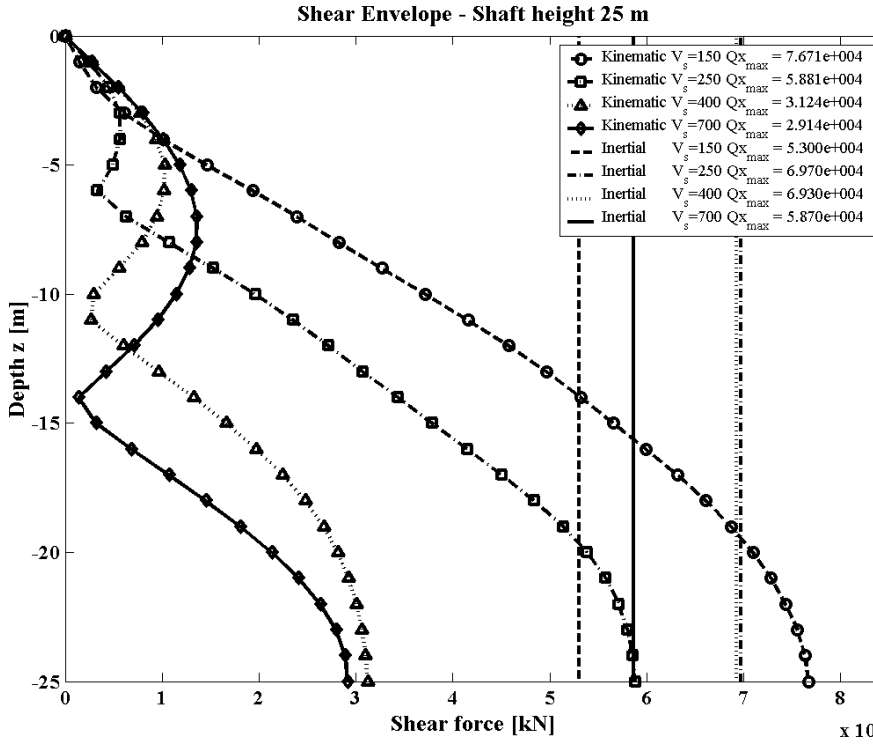

Fig. 16. Shear envelope profiles along a 25 m long shaft for the four categories of soil layers reported in Table 1. The contributions of kinematic and inertial interaction have been uncoupled.

Figures 16 and 17 clearly show that in soft soils (i.e. for V_S = 150–250 m/s) kinematic interaction is the main contributor in the profiles to internal actions whereas in stiff soil layers the situation is reversed. This is not surprising since in stiff soils the foundation movements are small and the superstructure behaves as if it were almost clamped at its base. Instead when the foundation is surrounded by a soft soil layer it may experience rigid-body motion which includes large displacements and rotations.

Another feature shown by Figs. 16 and 17 is that the largest values of internal actions originated by kinematic interaction occur at the foundation base. This result is somehow different from that observed in slender piles where the kinematic actions are usually concentrated at the interfaces of consecutive soil layers of sharply differing stiffness. In this case the maximum values (in absolute terms) of bending moment occur at intermediate sections of the pile length.

The fact that a large-diameter shaft foundation concentrates the maximum kinematic action at its base is a consequence of the degree of constraint that is developed at the end-base section which makes the foundation behaviour similar to a cantilever scheme, but opposite to the usual downward cap geometry.

6.4. *Results for foundation seismic capacity*

Kinematic interaction induces a complex system of soil dynamic pressures along the surface of the foundation shaft. Figures 18 and 19 show colour plots of the maximum normal (tensile) and tangential (shear) stresses occurring at the soil-foundation interface during the entire time-history of the excitation which is constituted by a simultaneous application of the East-West and North-South components of Duzce accelerograms from the 12/11/1999 Turkey earthquake. For a simultaneous application of two horizontal components of ground motion the total normal and shear stresses are obtained from the superposition principle (linear theory):

$$\sigma_r = \sigma_r^x \cos(\theta) + \sigma_r^y \sin(\theta), \quad \tau_{r\theta} = \tau_{r\theta}^x \sin(\theta) - \tau_{r\theta}^y \cos(\theta). \tag{23}$$

The tensile normal stress developed during earthquake shaking (i.e. $\sigma_r > 0$) plotted in Fig. 18 and the tangential circumferential stress exceeding the local interface shear capacity (i.e. $\tau_{r\theta} > \tau_{\text{lim}}$) illustrated in Fig. 19 are the most important indicators for assessing the seismic capacity of the foundation shaft. Another relevant parameter is the time of persistence of the above two stress conditions with respect to the total duration of seismic excitation. This piece of information allows to identify the most critical zones along the soil-foundation interface in light of the fact that it is not only important to verify if a given stress condition is violated but also, in engineering terms, for how long.

The parametric study performed for the viaduct shown in Fig. 12 put in evidence that for the shortest foundation (i.e. for $H = 15\,\text{m}$) the peak compressive normal stress exhibits a large dependence on soil categories with values ranging from $-150\,\text{kPa}$ (for $V_S = 700\,\text{m/s}$) to $-300\,\text{kPa}$ (for $V_S = 150\,\text{m/s}$). On the contrary, the deepest foundation (i.e. for $H = 35\,\text{m}$) displays a relatively high, constant peak compressive stress independently from soil category and approximately equal to $-400\,\text{kPa}$.

This trend is confirmed also for the peak tensile stress which ranges from 100 kPa (for $V_S = 150\,\text{m/s}$) to 30 kPa (for $V_S = 700\,\text{m/s}$) for the 15 m long shaft, and remains nearly constant and equal to 200 kPa for the 35 m long cylinder. Figure 18 shows clearly that the tensile stresses caused by the earthquake excitation are mostly concentrated at the top ring of the foundation where the displacements are large. The extension along the shaft of this critical zone increases with the increase of foundation length and it may persist in time for up to 30% of the total duration of the excitation. In short foundations the critical zone where $\sigma_r > 0$ is less extended and its persistence in time is more limited (in average about 10–20%).

Concerning the shear circumferential stress exceeding the local interface shear strength (i.e. $\tau_{r\theta} > \tau_{\text{lim}}$), Fig. 19 shows that similarly to the tensile stresses the critical zone is localised at the top ring of the foundation. However now the situation is more severe since the time interval over which the critical stress conditions are maintained is greater and in deep foundations it extends up to 60–80% of the total duration of earthquake excitation. Figure 19 shows that also for the peak shear

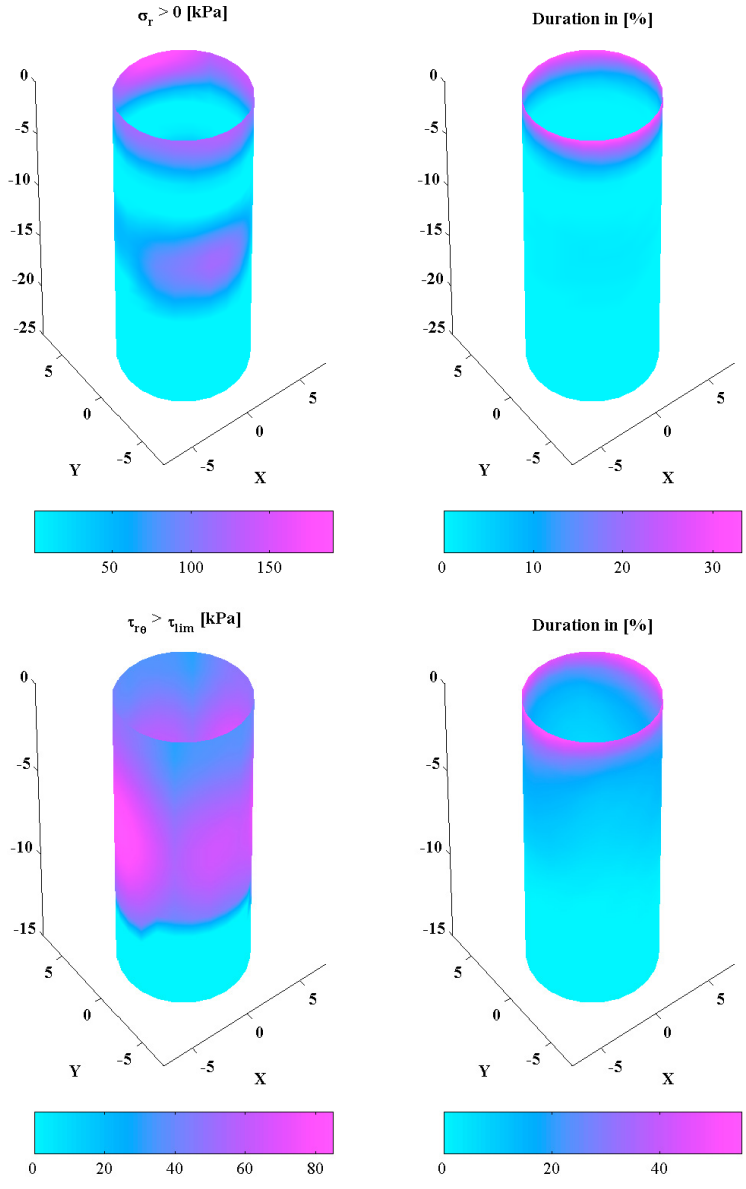

Fig. 17. Envelope of maximum normal tensile stress at the soil-foundation interface (left) and time of persistence as a percentage of duration of seismic excitation (right) (top — $H = 25\,\mathrm{m}$, $V_S = 400\,\mathrm{m/s}$; bottom — $H = 15\,\mathrm{m}$ $V_S = 250\,\mathrm{m/s}$).

stress the larger values are obtained in softer soil layers and for short foundation shafts. For a detailed account of all the results obtained from the parametric study of the bridge shown in Fig. 12 the interested reader is referred to the already mentioned work of Beltrami [2004] or Beltrami *et al.* [2005].

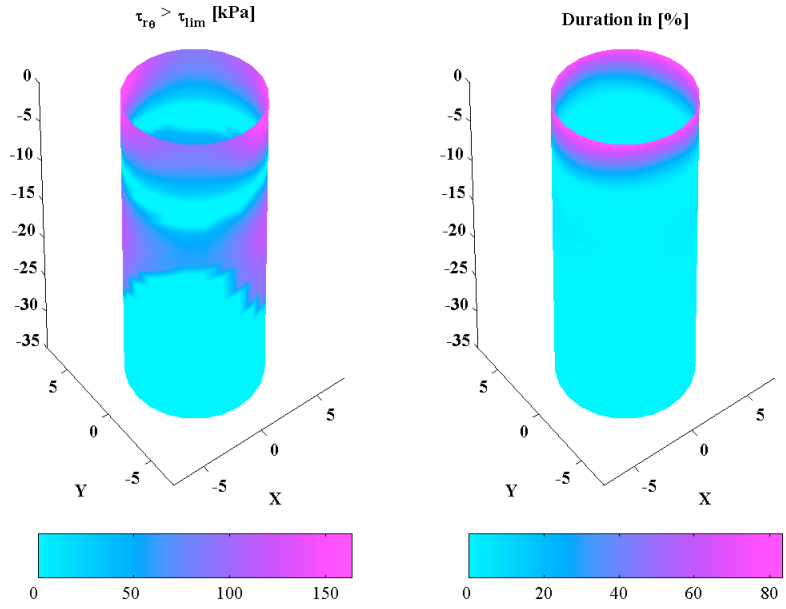

Fig. 18. Envelope of maximum tangential (shear) stress at the soil-foundation interface (left) and time of persistence as a percentage of duration of seismic excitation (right) ($H = 35\,\mathrm{m}$ $V_S = 400\,\mathrm{m/s}$).

7. Conclusions

This article illustrated the main features of an analytical model aimed to assess kinematic interaction in large-diameter shaft foundations. Although on the subject of kinematic interaction a large number of solutions are available for slender, flexible piles, relatively few solutions are available for deep, large-diameter shafts. The model is based on an extension to a deformable base of the solution obtained by Veletsos and Younan [1995] for fixed-base cylinders embedded in a linear, viscoelastic, homogeneous soil stratum. It has been further extended to inhomogeneous soil layers using the closed-form solution obtained by Pecker [2003, 2004] for one-dimensional ground response analysis in soil deposits where the shear wave velocity is a power function of depth with an arbitrary exponent. As a further generalisation, the kinematic interaction model for homogeneous soil layer has been extended to the case of a mixed "smooth" and "rough" soil-foundation interface.

The model has been developed using a fully analytical approach and it has been validated through a series of benchmark tests conducted with the finite element code SASSI. Despite the built-in simplifying assumptions the results obtained from the validation process are very satisfactory. The analytical solution of kinematic interaction presents a number of advantages over the corresponding numerical calculation. First it does not require any discretisation effort, as required for any finite element or finite difference code. Second the processing time is considerably reduced as it takes about 6 minutes to run an analysis with the analytical model and 1.5 hours

using the finite element code SASSI on the same machine. Another advantage of the theoretical model over numerical techniques is the flexibility it allows which allows the user to completely change the geometry of a problem without the need to re-define a mesh. Also the capability to simulate mixed "smooth" and "rough" boundary conditions at the soil-foundation interface constitutes an important characteristic of the kinematic model that is difficult to reproduce with a finite element code. These and other features make the proposed model ideal for applications in engineering practice, which was the original scope of this work: set-up a simplified though rigorous methodology to be used in engineering practice for assessing seismic soil-structure interaction in case of large-diameter shaft foundations.

The model has been applied to study the effects of kinematic interaction on a multi-span, continuous prestressed concrete viaduct with tall piers and large diameter piled foundations. The main finding of the study is the relevance of kinematic interaction in assessing the seismic response of structures founded on massive, rigid shafts. This is shown not only in terms of internal actions developed at the foundation level during seismic excitation (which are of the same order of magnitude of those induced by inertial interaction), but also for an increase of base-pier shear and moment demands. Both phenomena originate from the coupled swaying-rocking excitation caused by kinematic interaction and for which the foundation input motion (FIM) is characterised not only by a translational (horizontal) component but also a rotational part.

The parametric study conducted for the viaduct considering different soil categories showed that the most detrimental effects of kinematic interaction occur in soft soils because of the relevance of wave scattering effects.

In view of the most recent developments in seismic design where displacement-based approaches are growing in importance, the issue of rocking excitation at the base of a structure as a relevant component of seismic input is certain to receive a greater attention. For instance the displacement demand of a structure such as a tall bridge could be more accurately computed by superimposing the effects of both rotational and (horizontal) translational response spectra.

Further extensions of the kinematic interaction model illustrated in this article are currently under way. In particular attention is focused on extending the model to piled-foundations of rectangular sections, inhomogeneous soil layers having $V_S \neq 0$ at the free-surface, and accounting for phenomenon of kinematic vertical interaction.

Acknowledgements

The authors would like to express their gratitude to Prof. Eduardo Kausel of the Massachusetts Institute of Technology and to Dr. Roy A. Imbsen of Imbsen & Associates Inc. for providing valuable research reports for literature review on the subject. A word of gratitude goes also to Prof. Glenn Rix of the Georgia Institute of Technology for providing the article by Tajimi [1969].

References

Abrahamson, N. A. [1992] "Non-stationary spectral matching," *Seismological Research Letters* **63**(1), 30.

Abrahamson, N. A. and Silva, W. J. [1997] "Empirical response spectral attenuation relation for shallow crustal earthquakes," *Seismological Research Letters* **68**(1), 94–127.

ADINA 900 nodes version [2003] User's Manual, *Automatic Dynamic Incremental Nonlinear Analysis* — Version 8.0, K.J. Bathe — ADINA R & D Inc, USA.

Afra, H. and Pecker, A. [2002] "Calculation of free field response spectrum of a non-homogeneous soil deposit from bedrock response spectrum," *Soil Dynamics and Earthquake Engineering* **22**, 157–165.

Beltrami, C. [2004] *A Refined Methodology for Assessing Seismic Soil-Pile-Structure Interaction in Engineering Practice*, MSc Thesis, European School of Advanced Studies in Reduction of Seismic Risk, ROSE School, University of Pavia (Italy).

Beltrami, C., Lai, G. C. and Pecker, A. [2005] *Seismic Soil Structure Interaction in Large Diameter Shaft Foundations*, ROSE Research Report, European School of Advanced Studies in Reduction of Seismic Risk, ROSE School, IUSS Press, University of Pavia (Italy), (in press).

Bielak, J. [1975] "Dynamic behaviour of structures with embedded foundations," *Earthquake Engineering and Structural Dynamics* **3**, 259–274.

CALTRANS [1999] *Seismic Soil-Foundation-Structure Interaction*, Final Report, Prepared by The Caltrans Seismic Advisory Board — Ad Hoc Committee on Soil-Foundation-Structure Interaction, California Department of Transportation, Sacramento (CA).

Davis, R. O. and Hunt, B. [1994] "Amplification of vertically propagating SH waves by multiple layers of Gibson Soils," *Int. J. Numer. Anal. Methods in Geomech.* **18**, 205–212.

Dobry, R. and Gazetas, G. [1988] "Simple method for dynamic stiffness and damping of floating pile groups," *Géotechnique* **38**(4), 557–574.

Dobry, R., Oweis, I. and Urzua, A. [1976] "Simplified procedures for estimating the fundamental period of a soil profile," *Bulletin of the Seismological Society of America* **66**(4), 1293–1321.

El Naggar, M. H. and Bentley, K. J. [1999] "Dynamic analysis for laterally loaded piles and dynamic p-y curves," *Canadian Geotechnical Journal* **37**, 1166–1183.

Elsabee, F. and Morray, J. P. [1977] *Dynamic Behavior of Embedded Foundations*, Report No. R77-33, Dept. of Civil Eng., MIT, Cambridge, Massachusetts.

EUROCODE 8 [2003] *Design of Structures for Earthquake Resistance — Part 2: Bridges. Part 5: Foundations, Retaining Structures and Geotechnical Aspects*, Final Draft, European Standard, No. prEN 1998–5:2003 E.

Fenves, G. L. [2003] *Dynamic Analysis of Structures*, Lecture notes, ROSE School, Pavia, Italy.

Gazetas, G. [1984] "Seismic response of end-bearing single piles," *Soil Dynamics and Earthquake Engineering* **3**(2).

Kagawa, T. and Kraft, L. M., Jr. [1980] "Seismic p-y response of flexible piles," *Journal of the Geotechnical Engineering Division*, ASCE **106**(GT8), 899–918.

Kaul, M. K. [1978] "Spectra-consistent time-history generation," *Journal of the American Society of Civil Engineers*, ASCE **104**(EM4), 781–788.

Kausel, E., Whitman, V., Morray, J. P. and Elsabee, F. [1978] "The spring method for embedded foundations," *Nuclear Engineering and Design* **48**, 377–392.

Kavvadas, M. and Gazetas, G. [1993] "Kinematic seismic response and bending of free-head piles in layered soil," *Géotechnique* **43**(2), 207–222.

Kramer, S. L. [1996] *Geotechnical Earthquake Engineering*, Prentice Hall.

Lebedev, N. N. [1972] *Special Functions & Their Applications*, Dover Publications Inc., New York, USA.

Li, X. and Aguilar, O. [2000] "Elastic earth pressures on rigid walls under earthquake loading," *Journal of Earthquake Engineering* **4**(4), 415–435.

Lilhanand, K. and Tseng, W. S. [1988] "Development and application of realistic earthquake time histories compatible with multiple-damping design spectra," *Proc. of 9th World Conference on Earthquake Engineering*, August 2–9, Tokyo-Kyoto, Japan.

Mizuno, H. [1987] "Pile damage during earthquakes in Japan (1923–1983)," *Geotechnical Special Publication No. 11, Dynamic Response of Pile Foundations*, ASCE, pp. 53–78.

Mylonakis, G. and Gazetas, G. [2000] "Seismic soil-structure interaction: Beneficial or detrimental?" *Journal of Earthquake Engineering* **4**(3), 277–301.

Mylonakis, G., Nikolaou, A. and Gazetas, G. [1997] "Soil-pile-bridge seismic interaction: Kinematic and inertial effects. Part 1: Soft soil," *Earthquake Engineering and Structural Dynamics* **26**, 337–359.

Nikolau, S., Mylonakis, G., Gazetas, G. and Tazoh, T. [2001] "Kinematic pile bending during earthquakes: Analysis and field measurements," *Géotechnique* **51**(5), 425–440.

Nogami, T., Otani, J., Konagai, K. and Chen, H.-L. [1992] "Nonlinear soil-pile interaction model for dynamic lateral motion," *Journal of the Geotechnical Engineering*, ASCE **118**(1), January, 89–106.

Novak, M. and Aboul-Ella, F. [1978] "Impedance functions of piles in layered media," *Journal of the Engineering Mechanics Division* **104**(EM6), 641–661.

Novak, M., Sheta, M, El-Hifnawy, L., El-Marsafawi, H. and Ramadan, O. [1994] "DYNA4 a computer program for calculation of foundation response to dynamic loads," *Report No. GEOP 93-01*, User Manual, Vols. I and II, Geotechnical Research Centre, The University of Western Ontario, London, Ontario, Canada.

Pais, A. L. and Kausel, E. [1990] "Stochastic response of rigid foundations," *Earthquake Engineering and Structural Dynamics* **19**, 611–622.

PEER [2004] *Strong Motion Database*, http://peer.berkeley.edu/smcat/.

Pecker, A. [1984] "Dynamique des sols," *Presses de l'Ecole Nationale des Ponts et Chaussées*, Paris (France).

Pecker, A. [2002] *Soil Dynamics and Foundation Engineering*, Lecture notes, ROSE School, Pavia, Italy.

Pecker, A. [2003] "An estimate of maximum ground surface motion," *C. R. Mecanique* **331**, 661–666.

Pecker, A. [2004] "An estimate of maximum ground surface motion for non zero surface velocity," *C. R. Mecanique* **332/9**, 725–730.

Pecker, A. and Afra, H. [1995] "Charts for natural frequencies and transfer functions of inhomogeneous soil deposit," *5th International Conference on Seismic Zonation* **II**, 1091–1098.

Pender, M. J. [1993] "A seismic pile foundation design analysis," *Bull. New Zealand National Soc. Earthquake Eng.* **26**, 49–160.

Priestley, M. J. N., Seible, F. and Calvi, G. M. [1996] *Seismic Design and Retrofit of Bridges*," John Wiley & Sons, Inc.

Roesset, J. M. [1969] "Foundamentals of soil amplification," *Conference on Seismic Design for Nuclear Power Plants*, MIT, Robert J. Hansen (ed.), **1**, 183–244.

Roesset, J. M. and Kausel, E. [1976] "Dynamic soil structure interaction," *Numerical Methods in Geomechanics — ASCE*, C. S. Desai (ed.), **1**, 3–19.

SASSI 2000 [1999] User's Manual, *A System for Analysis of Soil-Structure Interaction — Revision 1.*

Schnabel, P., Lysmer, J. and Seed, H. B. [1972] Modified by Idriss I. M and Sun J. I. [1992] *User's Manual for SHAKE 91 — A Computer Program for Conducting Equivalent Linear Seismic Response Analyses of Horizontally Layered Soil Deposits*, Original Report No. UCB/EERC 72/12, Earthquake Engineering Research Center at University of California in Berkeley.

Schreyer, H. L. [1977] "One-dimensional elastic waves in inhomogeneous media," *Journal of the Engineering Mechanics Division — ASCE* **103**(EM5), 979–990.

Scott, R. F. [1973] "Earthquake-induced pressures on retaining walls," *Proc. 5th World Conf. Earthq. Eng.*, Rome, Italy **II**, 1611–1620.

Stewart, J., Seed, R. B. and Fenves, G. L. [1998] *Empirical Evaluation of Inertial Soil-Structure Interaction Effects*, Report PEER 98/07, November.

Tajimi, H. [1969] "Dynamic analysis of a structure embedded in elastic stratum," *Proc. 4th World Conference on Earthquake Engineering IAEE*, Santiago, Chile **III**(A-6), 53–69.

Veletsos, A. S. and Dotson, K. W. [1988] "Horizontal impedances for radially inhomogeneous viscoelastic soil layers," *Earthquake Engineering and Structural Dynamics* **16**, 947–966.

Veletsos, A. S. and Verbic, B. [1974] "Basic response functions for elastic foundation," *Journal of the Engineering Mechanics Division ASCE* **100**(EM2), April.

Veletsos, A. S. and Younan, A. H. [1994a] "Dynamic modelling and response of soil-wall systems," *Journal of Geotechnical Engineering ASCE* **120**(12), December.

Veletsos, A. S. and Younan, A. H. [1994b] "Dynamic soil pressures on rigid cylindrical vaults," *Earthquake Engineering and Structural Dynamics* **23**, 645–669.

Veletsos, A. S. and Younan, A. H. [1994c] "Dynamic soil pressures on rigid vertical walls," *Earthquake Engineering and Structural Dynamics* **23**, 275–301.

Veletsos, A. S. and Younan, A. H. [1995] "Dynamic modelling and response of rigid embedded cylinders," *Journal of Engineering Mechanics ASCE* **121**(9) September.

Wolf, J. P. [1994] *Foundation Vibration Analysis Using Simple Physical Models*, PTR Prentice Hall, NY, USA.

Wood, J. H. [1973] *Earthquake Induced-Pressures on Structures*, Report EERL 73-05, Earthquake Engineering Research Laboratory, California Institute of Technology.